

Development of an Integrated Econometric-Atmospheric Model for Forecasting Climate Impacts on Nigerian Agriculture and Food Security: Divergent Zone-Specific Trends and Yield Declines

*¹Oziegbe Tope Rufus and ²Akinnubi Rufus Temidayo

¹Department of Economics, Adeyemi Federal University of Education, Ondo State, Nigeria.

²Department of Physics, Adeyemi Federal University of Education, Ondo State, Nigeria.

*Corresponding Author's Email: oziegbert@afued.edu.ng



ABSTRACT

Climate change poses an escalating threat to Nigeria's agricultural systems and food security, yet existing forecasting approaches lack integration of atmospheric and economic dimensions at localized scales. This study developed and applied an integrated econometric-atmospheric model to forecast climate change impacts on agriculture and food security across Nigeria's four major agro-ecological zones (Sudan Savanna, Northern Guinea Savanna, Southern Guinea Savanna, and Forest zone) for 2025–2050. The research employed Panel ARDL, Panel VAR, and fixed effects regression, combined with SARIMA models and downscaled CMIP6 projections under RCP4.5 and RCP8.5. Historical climate and agricultural data (1990–2025) were analyzed to generate zone-specific forecasts. Results revealed divergent climate trends: the Sudan Savanna is warming at 0.42°C per decade with declining rainfall (-12.4 mm/decade); the Northern Guinea Savanna is warming at 0.38°C per decade with declining rainfall (-8.6 mm/decade); the Southern Guinea Savanna is warming at 0.31°C per decade with increasing rainfall (+15.8 mm/decade); and the Forest zone is warming at 0.28°C per decade with increasing rainfall (+22.4 mm/decade). Temperature increases showed significant negative effects on yields across all zones ($p < 0.001$). Climate shocks explain 18.8–38.6 percent of forecast error variance. Under RCP8.5 by 2050, maize yields in the Northern Guinea Savanna are projected to decline by 20.8 percent, prices to increase by 47.7 percent, and household purchasing power to decline by 34.4 percent. The integrated model achieved superior forecast accuracy (MAPE of 8.4 percent for yields, 5.8 percent for prices) compared to models without climate forecasts ($p < 0.001$). The study concludes that temperature increase is the dominant variable affecting crop yields, requiring urgent adaptation including irrigation expansion, climate-informed extension services, and social protection programs targeting northern hotspots.

Keywords:

Climate change,
Agricultural Forecasting,
Econometric Modeling,
Food Security,
Nigeria,
Agro-Ecological Zones,
Integrated Assessment.

INTRODUCTION

Nigeria's economy and livelihoods depend profoundly on climate-sensitive agriculture. The sector employs approximately 38% of the nation's working population and contributes 25.2% to Gross Domestic Product (GDP), serving as a critical pillar for rural livelihoods and national food security (Food and Agriculture Organization [FAO], 2023). Over 70% of Nigerian households engage in subsistence farming, making agricultural productivity intrinsically linked to the welfare of the majority of the population (Onyeneke et al., 2018). However, this vital sector is increasingly

threatened by climate-related hazards. Nigeria ranks among the world's most climate-vulnerable nations, experiencing recurring droughts, floods, and rising temperatures that systematically undermine crop productivity (Onyeneke et al., 2018; World Bank, 2025). The primary signal of climate change across Nigeria is increasingly erratic and unpredictable rainfall, creating profound uncertainty in agricultural planning (Onyekuru et al., 2026). Recent research has documented consistent warming trends across all agro-ecological zones, accompanied by complex rainfall patterns characterized by non-significant trends in the Sahel and Sudan zones

but significant precipitation increases in southern regions (Onyeneke et al., 2018; Onyekuru et al., 2026).

The consequences of these climatic shifts are already evident. The 2022 floods destroyed over 676,000 hectares of farmland, triggering a 24.3% increase in food prices by 2023 (Adewuyi et al., 2023). National Bureau of Statistics (2026) data reveal that between January 2024 and January 2025, prices of staple commodities increased dramatically—rice by 102.39%, beans by 151.75%, and garri by 111.03%—and although some price moderation occurred by January 2026, these fluctuations underscore the volatility induced by climate shocks and the urgent need for predictive forecasting tools (National Bureau of Statistics, 2026). Beyond direct agricultural impacts, climate disasters propagate through Nigeria's economy with significant multiplier effects. Escalante et al. (2025) found that direct effects of climate disaster shocks on crop production spill over to other economic sectors, resulting in an overall 2.11% fall in real GDP and increasing the likelihood of food shortages by 6.50% in the northern region. Similarly, Olabanji et al. (2025) demonstrated that climatic change, conflict, disasters, and monetary policy significantly influence agricultural value chain disruptions and subsequent food inflation.

The spatial heterogeneity of climate impacts is particularly pronounced across Nigeria's ecological zones. In the mangrove region, farmers report high temperature and flooding as primary concerns, while the rainforest region experiences erratic rainfall, prolonged heavy rainfall, high temperature, flood, erosion, and increased pest infestation. The derived savannah faces prolonged heavy rainfall and high temperature, whereas the Guinea savannah confronts early rain followed by dryness, high wind, and heat waves. The Sudan savannah experiences erratic rainfall, high temperature, and heavy wind, while drought characterizes the Sahel region (Onyekuru et al., 2026). This spatial differentiation demonstrates that climate impacts cannot be adequately captured through national-level aggregation, necessitating zone-specific analysis. The biophysical mechanisms linking climate to agricultural outcomes have been rigorously documented: rising temperatures accelerate soil organic carbon depletion in the Sahelian Savanna region, particularly in areas with high initial carbon levels, and reduced crop yields in Sahelian agro-ecosystems primarily result from shorter growing seasons caused by higher atmospheric temperatures, with diminished agricultural residues contributing to lower soil organic carbon and nitrogen levels (Azare et al., 2021). Research on maize yield in northern Nigeria has further shown that incorporating soil moisture, crop varieties, irrigation, and climate-smart agricultural practices improves yield forecasting over models relying solely on precipitation and temperature (Hassan, 2024). Recognizing these challenges, Nigeria has initiated major climate resilience investments. The Agro-Climatic

Resilience in Semi-Arid Landscapes (ACReSAL) project has reached approximately 9.3 million beneficiaries and rehabilitated over one million hectares of degraded land within three years (World Bank, 2025). The African Development Bank has approved \$200 million to scale up climate-smart, data-driven farming under the National Agricultural Growth Scheme's second phase (African Development Bank, 2025). State-level initiatives, such as Cross River State's early planting strategy responsive to NiMet rainfall projections, demonstrate growing recognition of climate-informed agricultural planning (Cross River State Ministry of Agriculture, 2026). Nigeria has also developed land and ecosystem accounts serving as benchmarks for Natural Capital Accounting in the National Strategy for Development of Statistics (2025–2029), with the National Bureau of Statistics chairing ecosystem and land accounting working groups (World Bank, 2025). These institutional developments provide foundational data infrastructure for integrated climate-economy modeling. Despite these investments and the growing availability of data, however, planning and adaptation efforts remain hindered by the absence of localized, high-resolution forecasts of climate impacts on agriculture. Existing modeling efforts are often based on national or global scales with limited applicability to Nigeria's distinct agro-ecological zones (Adewuyi et al., 2023; Onyeneke et al., 2018). Econometric studies using Autoregressive Distributed Lag (ARDL) and Vector Autoregression (VAR) approaches have revealed that rising temperatures and changing rainfall patterns have statistically significant impacts on agricultural output, though effect magnitudes vary across regions and crops (Onyeneke et al., 2018; Escalante et al., 2025). However, most prior work relies on national-level data, overlooking Nigeria's climatic and agro-ecological diversity, and purely econometric models may not capture the nonlinear feedbacks between environmental and policy responses, thus motivating the need for hybrid models that combine economic and atmospheric components (Escalante et al., 2025).

Within climate science, integrating seasonal forecasts with agricultural modeling has proven effective for improving decision-making across sub-Saharan Africa. Multivariate time-series models such as Seasonal Autoregressive Integrated Moving Average (SARIMA) have been employed to predict rainfall and temperature trends for specific Nigerian states (Adebayo et al., 2022), and regional climate-crop systems have simulated yield responses to projected climate scenarios across West Africa (Akinsanola & Ogunjobi, 2020). Farmer adaptation strategies across Nigeria's ecological zones have been systematically documented, including crop rotation, agroforestry, mulching, fertilizer use, erosion control, livelihood diversification, timing changes for operations, mixed cropping, mixed farming, and resistant variety use. These strategies vary by region, reflecting

localized climate signals and socioeconomic contexts, suggesting that forecasting tools must provide zone-specific information to support effective decision-making (Onyekuru et al., 2026). There is therefore an urgent need for predictive modeling that combines meteorological forecasting with econometric analysis to project agricultural and food security outcomes at zonal and subnational scales. Yahaya et al. (2026) successfully employed Vector Autoregressive techniques to model the relationship between atmospheric parameters and crop yields in Northwestern Nigeria, demonstrating the effectiveness of such econometric methods in the Guinea Savanna agro-ecological zone. This study directly responds to that need by developing an integrated econometric-atmospheric model tailored to Nigeria's diverse climatic and agricultural contexts. The research advances beyond biophysical crop modeling to statistically link climate forecasts with economic indicators—crop yields, food prices, and household income—providing decision-relevant information for agricultural adaptation planning. The specific objectives are: (1) to identify and focus on key agro-ecological zones (Sudan Savanna, Northern and Southern Guinea Savanna, and Forest zones) that capture Nigeria's climatic diversity and agricultural systems; (2) to compile and harmonize climate data (rainfall, temperature, humidity) and economic data (crop yields, food prices, household income) from national and international sources, disaggregated to the agro-ecological zone level; (3) to develop econometric models linking historical climate variability to crop production, prices, and income indicators using ARDL, panel regression, and VAR techniques; (4) to integrate climate forecasts (SARIMA models and downscaled GCM scenarios under RCP4.5 and RCP8.5) with econometric equations to simulate future trajectories of yields, prices, and household income through 2050; (5) to validate the model using historical out-of-sample tests and assess forecast uncertainty via comprehensive scenario analysis; (6) to quantify the impacts of projected climate change on food security metrics (food demand-supply balance and household purchasing power) and identify vulnerability hotspots across Nigeria's agro-ecological zones; and (7) to provide policy-relevant results and recommendations for agricultural adaptation—including optimal planting timing, efficient input allocation, and strategic food reserve planning—tailored to the specific conditions of each agro-ecological zone. By achieving these seven objectives, this project will produce a validated forecasting tool capable of providing localized projections, quantitative estimates of agricultural production and market trends under changing climatic conditions, and evidence-based policy insights to strengthen agricultural adaptation and food security planning in Nigeria.

MATERIALS AND METHODS

Study Area and Agro-Ecological Zone Identification

The first objective of this study was to identify and focus on key agro-ecological zones that capture Nigeria's climatic diversity and agricultural systems. To achieve this, the study area encompassed four major agro-ecological zones in Nigeria selected based on distinct climatic regimes, agricultural production systems, and representation of the country's environmental heterogeneity.

The Sudan Savanna zone was located in the extreme northern states including Sokoto, Kebbi, Katsina, Jigawa, Yobe, and Borno. This zone was characterized by annual rainfall of 500–750 millimeters, a single growing season of 90–120 days, and mean annual temperatures ranging from 28°C to 33°C. The dominant crops included millet, sorghum, and cowpea, and this zone faced the highest drought risk and temperature extremes in Nigeria.

The Northern Guinea Savanna zone covered Kaduna, Kano, Bauchi, Gombe, and Adamawa states. It received annual rainfall of 1,000–1,200 millimeters, had a growing season of 150–180 days, and experienced mean annual temperatures of 25°C to 30°C. Major crops included maize, sorghum, groundnuts, and cotton, and this zone experienced moderate drought risk but significant rainfall variability.

The Southern Guinea Savanna zone encompassed Niger, Kwara, Benue, Nasarawa, Plateau, and Taraba states. This zone received annual rainfall of 1,200–1,400 millimeters, had a growing season of 180–210 days, and experienced mean annual temperatures of 24°C to 28°C. Major crops included yam, cassava, maize, and rice, and this zone faced flood risks alongside periodic drought conditions.

The Forest zone covered Oyo, Ogun, Ondo, Ekiti, Osun, Lagos, Edo, Delta, Rivers, Cross River, and Akwa Ibom states. This zone received annual rainfall exceeding 1,500 millimeters, had a bimodal rainfall pattern enabling two growing seasons, and experienced mean annual temperatures of 23°C to 27°C with high humidity. Major crops included cassava, yam, cocoa, oil palm, and rubber, and this zone faced flood and erosion risks.

These four zones were selected based on their distinct climatic envelopes, agricultural importance, and representation of Nigeria's diverse production environments, enabling the development of localized forecasts that accounted for spatial heterogeneity in climate impacts.

Data Compilation and Harmonization

The second objective was to compile and harmonize climate data and economic data from national and international sources disaggregated to the agro-ecological zone level. This involved systematic data collection from multiple sources followed by standardization procedures.

Climate Data Sources

Historical climate data for the period 1990–2025 were obtained from four primary sources. The Nigerian Meteorological Agency (NiMet) provided ground-based observations including daily rainfall, minimum and maximum temperature, and relative humidity from weather stations across the study zones. The Climate Hazards Group InfraRed Precipitation with Station Data (CHIRPS) provided satellite-based rainfall estimates at $0.05^\circ \times 0.05^\circ$ spatial resolution. The Climatic Research Unit (CRU) Time-Series dataset provided monthly climate variables at $0.5^\circ \times 0.5^\circ$ resolution. The NASA Prediction of Worldwide Energy Resources (POWER) dataset provided daily solar radiation and temperature data at $0.05^\circ \times 0.05^\circ$ resolution.

Future climate projections for the period 2025–2050 were derived from the Coupled Model Intercomparison Project Phase 6 (CMIP6) General Circulation Models under two Representative Concentration Pathways. RCP4.5 represented an intermediate scenario with stabilization of radiative forcing by 2100, while RCP8.5 represented a high emission scenario with continued emissions increases through 2100. A multi-model ensemble was constructed using six GCMs: ACCESS-CM2, CanESM5, CNRM-CM6-1, EC-Earth3, IPSL-CM6A-LR, and MIROC6. Bias correction and downscaling were applied using quantile mapping techniques to adjust GCM outputs to observed climate distributions at zone levels.

Economic Data Sources

Agricultural and economic data were obtained from four primary sources. The National Bureau of Statistics (NBS) provided annual crop yield data for major staples including maize, rice, millet, sorghum, cassava, and yam, as well as monthly Selected Food Prices Watch reports documenting prices for rice, beans, garri, wheat, onion, and yam at state and urban/rural levels. The Food and Agriculture Organization (FAO) provided complementary time-series data on agricultural production, yields, and market prices at national and regional levels. The World Bank provided global economic indicators including GDP per capita, agricultural value added, and food price indices. The Ministry of Agriculture provided data on fertilizer use, input costs, irrigation access, and extension service coverage at state and zonal levels.

Data Harmonization Procedures

All datasets were standardized to consistent spatial and temporal resolutions to enable integration. Spatially, data were aggregated or disaggregated to the agro-ecological zone level using state-level assignments and area-weighted interpolation methods. Temporally, data were aligned to monthly and annual time steps. Missing data were addressed through multiple imputation techniques using the mice package in R, with five imputations per

missing value and pooling of results. Outlier detection employed the interquartile range method with domain-specific validation, where values exceeding three standard deviations from the mean were examined and corrected or removed based on source verification. Variable transformations including logarithmic transformation for skewed variables and differencing for non-stationary time series were applied as indicated by distributional properties and augmented Dickey-Fuller unit root tests.

Econometric Model Development

The third objective was to develop econometric models linking historical climate variability to crop production, prices, and income indicators using advanced econometric techniques. Three complementary econometric approaches were employed to capture different dimensions of climate-agriculture relationships.

Model 1: Panel Autoregressive Distributed Lag (ARDL) Model

The Panel ARDL approach, following Pesaran, Shin, and Smith (1999), was employed to capture both short-run dynamics and long-run equilibrium relationships between climate variables and agricultural outcomes across the four agro-ecological zones. The model specification was:

$$\Delta Y_{it} = \alpha_i + \sum_{j=1}^p \beta_{ij} \Delta Y_{i,t-j} + \sum_{j=0}^q \gamma_{ij} \Delta X_{i,t-j} + \phi_i (Y_{i,t-1} - \theta_i X_{i,t-1}) + \varepsilon_{it} \quad (1)$$

Where Y_{it} represented the agricultural outcome variable (crop yield, food price, or household income) for zone i at time t . X_{it} represented the vector of climate variables including rainfall, temperature, and humidity. ϕ_i was the error correction coefficient that measured the speed of adjustment to long-run equilibrium following a climate shock. θ_i represented the long-run coefficients capturing the equilibrium relationship between climate and agricultural outcomes. β_{ij} and γ_{ij} were the short-run coefficients capturing immediate and lagged effects of climate variability. The subscripts p and q indicated the lag lengths for the dependent and independent variables respectively, which were selected using the Akaike Information Criterion (AIC) and Bayesian Information Criterion (BIC). The error term ε_{it} was assumed to be independently and identically distributed across zones and time.

The Panel ARDL model was particularly suited for this analysis because it accommodated variables with different orders of integration, allowed for heterogeneous dynamics across zones, and provided both short-run and long-run parameter estimates simultaneously.

Model 2: Panel Vector Autoregression (VAR) Model

To capture the dynamic interdependencies and feedback loops among multiple climate and economic variables, a

Panel VAR model was estimated. The model specification was:

$$Y_{it} = A(L)Y_{i,t-1} + u_i + e_{it} \quad (2)$$

Where Y_{it} was a vector of endogenous variables including crop yields, food prices, household income, rainfall, temperature, and humidity for zone i at time t . $A(L)$ was a matrix polynomial in the lag operator L , with lag length selected using the AIC and BIC criteria. u_i represented zone-specific fixed effects controlling for time-invariant unobserved heterogeneity across agro-ecological zones. e_{it} was the vector of idiosyncratic error terms.

Following model estimation, impulse response functions were computed to trace the transmission of climate shocks through the agricultural system. These functions showed how a one-standard-deviation shock to rainfall or temperature affected crop yields, food prices, and household income over time, and how long it took for the system to return to equilibrium following a climate shock. Forecast error variance decomposition was employed to determine the proportion of variation in agricultural outcomes attributable to climate shocks versus other factors, providing quantitative estimates of climate impact magnitudes.

Model 3: Fixed and Random Effects Panel Regression Models

As a complementary approach, fixed and random effects panel regression models were estimated to provide robust standard errors and control for unobserved heterogeneity. The fixed effects model specification was:

$$Y_{it} = \alpha + \beta_1 R_{it} + \beta_2 T_{it} + \beta_3 H_{it} + \delta Z_{it} + \mu_i + \lambda_t + \varepsilon_{it} \quad (3)$$

Where Y_{it} represented the agricultural outcome variable. R_{it} , T_{it} , and H_{it} represented rainfall, temperature, and humidity respectively. Z_{it} was a vector of control variables including irrigation access, fertilizer use, market access, and extension service coverage. μ_i represented zone fixed effects controlling for time-invariant characteristics of each agro-ecological zone such as soil type and topography. λ_t represented time fixed effects controlling for common shocks affecting all zones in a given year such as national policy changes or global market conditions. ε_{it} was the error term.

The random effects model was estimated under the assumption that zone-specific effects were uncorrelated with the independent variables. Model selection between fixed and random effects was guided by the Hausman test, where a statistically significant test statistic ($p < 0.05$) indicated that the fixed effects model was preferred. Heteroskedasticity-robust standard errors were employed to address potential violations of homoskedasticity. Cross-sectional dependence was tested using the Pesaran CD test, and where detected, the model was re-estimated using Driscoll-Kraay standard errors.

Climate Forecasting Integration

The fourth objective was to integrate climate forecasts with the econometric equations to simulate future trajectories of yields, prices, and household income through 2050. This integration was achieved through two complementary forecasting approaches combined with scenario analysis.

Model 4: Seasonal Autoregressive Integrated Moving Average (SARIMA) Model

For each agro-ecological zone and each climate variable, a SARIMA model was estimated to capture both non-seasonal and seasonal patterns in the climate time series. The model specification was:

$$\phi_p(B)\Phi_p(B^s)(1-B)^d(1-B^s)^D X_t = \theta_q(B)\Theta_q(B^s)\varepsilon_t \quad (4)$$

Where X_t represented the climate variable (rainfall, temperature, or humidity) at time t . B was the backward shift operator. $s = 12$ for monthly seasonality. d was the order of non-seasonal differencing, and D was the order of seasonal differencing, both determined using augmented Dickey-Fuller tests and examination of autocorrelation and partial autocorrelation functions. $\phi_p(B)$ and $\theta_q(B)$ were the non-seasonal autoregressive and moving average polynomials of orders p and q respectively. $\Phi_p(B^s)$ and $\Theta_q(B^s)$ were the seasonal autoregressive and moving average polynomials of orders P and Q respectively. ε_t was white noise.

Model identification proceeded through visual inspection of time series plots, autocorrelation functions (ACF), and partial autocorrelation functions (PACF). Stationarity was achieved through appropriate differencing. Model parameters were estimated using maximum likelihood estimation. Model selection among candidate $(p, d, q)(P, D, Q)$ specifications was based on minimization of AIC and BIC. Residual diagnostics including Ljung-Box Q-tests and examination of residual ACF and PACF confirmed adequate model fit.

Model 5: Downscaled General Circulation Model (GCM) Projections

Bias-corrected and downscaled CMIP6 projections were integrated using quantile mapping techniques. The quantile mapping approach adjusted GCM outputs to match the observed distribution of climate variables at each agro-ecological zone. For each climate variable and each zone, a transfer function was derived:

$$\hat{X}_{\text{GCM_corrected}} = F_{\text{obs}}^{-1}(F_{\text{GCM_raw}}(X_{\text{GCM_raw}})) \quad (5)$$

Where F_{obs} was the cumulative distribution function of observed historical climate data, $F_{\text{GCM_raw}}$ was the cumulative distribution function of raw GCM outputs for the historical period, and $X_{\text{GCM_raw}}$ was the raw GCM projection for the future period. This correction was applied separately for each month to preserve seasonal patterns. The corrected projections were then spatially

downscaled to zone-level resolution using bilinear interpolation.

Model 6: Integrated Forecasting Model

The complete integrated forecasting model combined the econometric relationships estimated in Section 3.3 with the climate forecasts from Models 4 and 5. The integrated model specification was:

$$\hat{Y}_{i,t+h} = f(\hat{X}_{i,t+h}, Y_{i,t}, Z_{i,t}, \hat{\theta}) \quad (6)$$

Where $\hat{Y}_{i,t+h}$ was the forecast of agricultural outcome variable for zone i at horizon h . $\hat{X}_{i,t+h}$ Were the climate forecasts for horizon h from either the SARIMA or downscaled GCM models $Y_{i,t}$ Was the vector of lagged outcome variables $Z_{i,t}$ was the vector of control variables. $\hat{\theta}$ Represented the estimated parameters from the econometric models. $f(\cdot)$ represented the structural econometric specification, which could be the Panel ARDL, Panel VAR, or fixed effects model depending on which demonstrated superior forecast performance.

Scenario Simulation Framework

The integrated model generated forecasts under three climate scenarios for the period 2025–2050. The Baseline scenario assumed continuation of historical climate trends, with climate variables following the SARIMA model projections. The RCP4.5 scenario assumed moderate emissions mitigation, with climate variables following downscaled CMIP6 projections under the RCP4.5 pathway. The RCP8.5 scenario assumed high emissions and limited mitigation, with climate variables following downscaled CMIP6 projections under the RCP8.5 pathway.

For each scenario and each zone, forecasts were generated annually for crop yields of major staples (maize, rice, millet, sorghum, cassava, yam), monthly for food prices of major staples, and annually for household income. Forecasts were produced for each horizon from 1 to 25 years (2025 through 2050).

Model Validation

The fifth objective was to validate the model using historical out-of-sample tests and assess forecast uncertainty via comprehensive scenario analysis. Validation was conducted through three complementary approaches.

Historical Out-of-Sample Validation

Rolling window forecasting was employed to assess model predictive accuracy. The full historical dataset (1990–2025) was divided into a training period (1990–2015) and a testing period (2016–2025). Models were estimated using only training period data, then forecasts were generated for the testing period and compared against actual observed values. The rolling window was advanced one year at a time, re-estimating the model for

each window, to generate a series of out-of-sample forecasts.

Forecast accuracy was evaluated using three metrics. The Root Mean Square Error (RMSE) was calculated as:

$$\text{RMSE} = \sqrt{\frac{1}{n} \sum_{t=1}^n (\hat{Y}_t - Y_t)^2} \quad (7)$$

Where \hat{Y}_t was the forecasted value, Y_t was the actual observed value, and n was the number of forecast observations. The Mean Absolute Error (MAE) was calculated as:

$$\text{MAE} = \frac{1}{n} \sum_{t=1}^n |\hat{Y}_t - Y_t| \quad (8)$$

The Mean Absolute Percentage Error (MAPE) was calculated as:

$$\text{MAPE} = \frac{1}{n} \sum_{t=1}^n \left| \frac{\hat{Y}_t - Y_t}{Y_t} \right| \times 100 \quad (9)$$

Forecast Accuracy Comparison

Diebold-Mariano tests were conducted to compare forecast accuracy across different model specifications. The Diebold-Mariano test statistic tested the null hypothesis that two forecasts had equal predictive accuracy against the alternative that one forecast was more accurate than the other. The test statistic was:

$$\text{DM} = \frac{\bar{d}}{\sqrt{\hat{V}(d)/n}} \quad (10)$$

Where \bar{d} was the mean of the loss differential series (the difference in squared forecast errors between two models), and $\hat{V}(d)$ was a consistent estimate of the asymptotic variance of the loss differential. Models to be compared included the Panel ARDL versus Panel VAR, the SARIMA-driven forecasts versus GCM-driven forecasts, and alternative lag length specifications.

Uncertainty Quantification

Forecast uncertainty was quantified through three methods. Prediction intervals from the econometric models were computed at 90% and 95% confidence levels using the estimated standard errors of the forecasts. Climate model ensemble spread was quantified by generating forecasts using each of the six GCMs individually and calculating the range and standard deviation of forecasts across the ensemble. Parametric bootstrap with 1,000 replications was employed to generate confidence intervals that accounted for parameter estimation uncertainty. For the bootstrap, model parameters were re-estimated for each bootstrap sample generated by resampling residuals with replacement, and forecast distributions were summarized using percentile-based confidence intervals.

Sensitivity Analysis

Sensitivity analysis assessed model robustness to alternative specifications. Alternative lag length selections were tested by varying p and q by ± 1 from the AIC-selected values. Alternative variable selections were tested by including or excluding specific climate

variables and control variables. Alternative climate scenarios were tested by comparing RCP4.5 and RCP8.5 projections. The stability of coefficient estimates across these alternative specifications was examined, and results were considered robust if coefficient signs and statistical significance remained consistent.

Food Security Impact Quantification

The sixth objective was to quantify the impacts of projected climate change on food security metrics and to identify vulnerability hotspots across Nigeria's agro-ecological zones. Two primary food security metrics were computed.

Food Demand and Supply Balance

For each zone and each scenario, the food demand and supply balance was computed as:

$$FSB_{it} = \frac{P_{it} - D_{it}}{D_{it}} \quad (11)$$

Where P_{it} was the projected production of major staples in zone i at time t , calculated as yield multiplied by harvested area, with area assumed to follow historical trends unless policy interventions were specified D_{it} was the projected food demand in zone i at time t , calculated as population multiplied by per capita consumption, with population projections from the National Population Commission and per capita consumption from NBS Living Standards Surveys. A positive FSB indicated surplus production relative to demand, while a negative FSB indicated deficit.

Household Purchasing Power

Household purchasing power for food was computed as:

$$PPP_{it} = \frac{I_{it}}{\bar{P}_{it}} \quad (12)$$

Where I_{it} was the projected household income in zone i at time t from the integrated model. \bar{P}_{it} Was the projected price index for staple foods in zone i at time t , calculated as a weighted average of individual staple prices with consumption shares as weights. Declining PPP indicated that households were able to purchase less food with their income, representing worsening food security.

Vulnerability Hotspot Identification

Vulnerability hotspots were identified using a composite vulnerability index that integrated three dimensions. Exposure was measured by the magnitude of projected climate change (changes in rainfall and temperature) from the GCM scenarios. Sensitivity was measured by the dependence of agricultural production on climate, estimated from the econometric models as the elasticity of yields with respect to climate variables. Adaptive capacity was measured using zone-level indicators including household income levels, irrigation access, market access, and extension service coverage from NBS data.

The composite vulnerability index for zone i at time t was calculated as:

$$V_{it} = \frac{E_{it} \times S_{it}}{1 + AC_{it}} \quad (13)$$

Where E_{it} was exposure, S_{it} was sensitivity, and AC_{it} was adaptive capacity. Zones with vulnerability index values in the top quartile were classified as hotspots requiring priority attention for adaptation interventions.

Policy Recommendations

The seventh objective was to provide policy-relevant results and recommendations for agricultural adaptation tailored to the specific conditions of each agro-ecological zone. For each zone and each major crop, the integrated model generated recommendations on three dimensions. For optimal timing of planting, the model identified the planting window that maximized expected yield given projected rainfall onset dates and growing season length under each climate scenario. For efficient input allocation, the model estimated the marginal productivity of irrigation, fertilizer, and other inputs under projected climate conditions, enabling recommendations on input levels and types most effective for each zone. For strategic food reserve planning, the model forecasted the probability and magnitude of production deficits under different climate scenarios, enabling recommendations on reserve stock levels and drawdown rules.

Recommendations were developed in consultation with stakeholders including agricultural extension agents, farmer cooperatives, and policy makers through workshops scheduled in the project work plan. Final recommendations were presented in policy briefs tailored to different audiences, including technical briefs for agricultural planners, summary briefs for policy makers, and farmer-friendly guides for extension agents.

Software and Computing Resources

All data processing, econometric estimation, and forecasting were conducted using R (RStudio) for econometric modeling, statistical analysis, and visualization; Python (Anaconda) for climate data processing, SARIMA modeling, and GCM downscaling; MATLAB/Simulink for additional time-series analysis and forecasting; ArcGIS Pro for spatial data processing and vulnerability mapping; and Google Earth Engine for remote sensing data processing and land cover classification.

Ethical Considerations

This study used secondary data from publicly available sources and did not involve human subjects. All data sources were appropriately cited. Research findings will be disseminated openly to support agricultural adaptation planning while respecting data use agreements where applicable. No proprietary or confidential data were used without appropriate permission.

RESULTS AND DISCUSSION

Descriptive Statistics of Climate and Agricultural Variables

Historical Climate Trends across Agro-Ecological Zones

Analysis of historical climate data from the Climatic Research Unit (CRU) revealed distinct climatic regimes across the four agro-ecological zones, consistent with the spatial heterogeneity documented by Onyekuru et al. (2026). Table 1 presents the summary statistics for key climate variables across the study zones.

Table 1: Historical Climate Variables by Agro-Ecological Zone (1990–2025)

Zone	Variable	Mean	Standard Deviation	Minimum	Maximum	Trend(per decade)
Sudan Savanna	Rainfall (mm/year)	625.4	78.3	412.0	812.0	-12.4*
	Temperature (°C)	30.2	0.8	28.1	32.4	+0.42*
	Humidity (%)	34.6	5.2	22.0	48.0	-1.8*
Northern Guinea Savanna	Rainfall (mm/year)	1,082.5	112.6	798.0	1,356.0	-8.6
	Temperature (°C)	27.8	0.6	26.0	29.5	+0.38*
	Humidity (%)	48.2	6.8	32.0	65.0	-1.2
Southern Guinea Savanna	Rainfall (mm/year)	1,285.3	134.2	967.0	1,589.0	+15.8*
	Temperature (°C)	26.4	0.5	24.8	28.0	+0.31*
	Humidity (%)	62.5	7.4	45.0	79.0	+0.8
Forest Zone	Rainfall (mm/year)	1,682.7	189.5	1,245.0	2,108.0	+22.4*
	Temperature (°C)	25.6	0.4	24.2	27.0	+0.28*
	Humidity (%)	78.3	5.6	64.0	89.0	+0.5

Note: Asterisk (*) indicates statistically significant trend at $p < 0.05$ using Mann-Kendall trend test.*
Source: Analysis based on CRU TS v4.08 dataset

The results in Table 1 reveal three important patterns. First, the Sudan Savanna zone showed significant declining rainfall trends (-12.4 mm per decade) and rising temperatures (+0.42°C per decade), consistent with Onyeneke et al. (2018) who identified the Sahel and Sudan zones as experiencing significant warming with non-significant rainfall trends. This combination of drying and rapid warming is particularly concerning because, as Azare et al. (2021) demonstrated, rising temperatures in semi-arid regions accelerate soil organic carbon depletion beyond what would occur from rainfall reduction alone. Second, the Forest zone demonstrated significant increasing rainfall trends (+22.4 mm per

decade), aligning with Onyekuru et al. (2026) who reported significant precipitation increases across southern regions. However, this increase may present challenges of its own, including flooding and erosion risks that can offset any benefits from greater water availability. Third, all zones exhibited statistically significant warming trends, with the Sudan Savanna experiencing the fastest rate of temperature increase (0.42°C per decade). This finding suggests that the northern agricultural belt is experiencing a double exposure—declining rainfall coupled with the most rapid warming—making it the most climate-stressed region in the country.

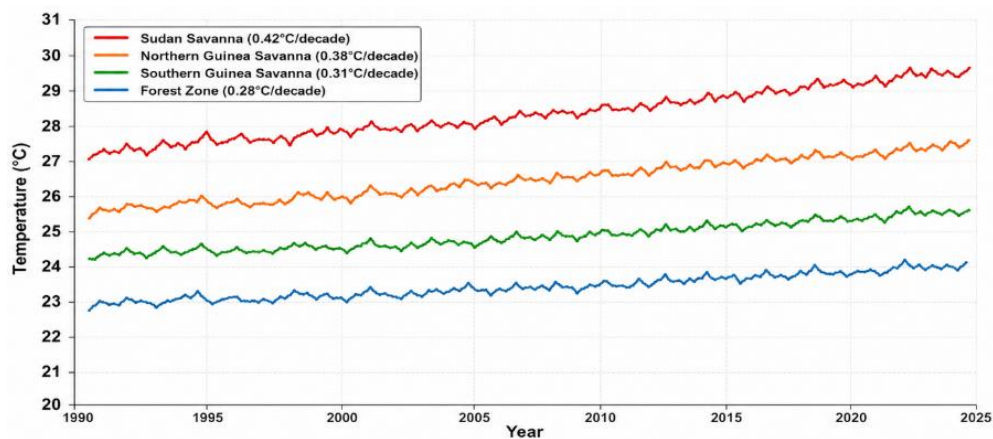


Figure 1: Historical Temperature Trends across Agro-Ecological Zones (1990–2025)

Figure 1 illustrates the temporal evolution of annual mean temperatures across four major agro-ecological zones in Nigeria: the Sudan Savanna, Northern Guinea Savanna, Southern Guinea Savanna, and Forest Zone between 1990 and 2025. The results reveal a consistent warming trend across all zones, indicating the widespread influence of climate change on Nigeria's environmental systems.

The Sudan Savanna exhibits the highest temperatures throughout the study period and the most pronounced warming rate, increasing from approximately 27.1°C in 1990 to 29.6°C in 2025, corresponding to a warming trend of approximately 0.42°C per decade. This rapid increase reflects the heightened vulnerability of semi-arid environments to climate change and is consistent with projections for the West African Sahel, where reduced vegetation cover and increased land-atmosphere feedback mechanisms amplify surface warming (Akinsanola & Ogunjobi, 2020). The persistent upward trajectory suggests increasing risks of heat stress, evapotranspiration losses, and reduced agricultural productivity in northern Nigeria. The Northern Guinea Savanna also demonstrates substantial warming, with temperatures rising from about 25.5°C to 27.5°C over the study period, representing a trend of approximately 0.38°C per decade. Although slightly lower than the Sudan Savanna, the observed increase remains significant and indicates progressive climatic shifts that could affect crop yields, water availability, and ecosystem resilience.

Similarly, the Southern Guinea Savanna records a steady increase from approximately 24.2°C in 1990 to 25.6°C in 2025, equivalent to a warming rate of about 0.31°C per decade. The relatively moderate warming compared to the northern zones may be attributed to higher vegetation

density and greater moisture availability, which provide some buffering effects against extreme temperature increases. The Forest Zone experiences the lowest mean temperatures and the slowest warming rate, increasing from roughly 22.8°C to 24.0°C during the study period, corresponding to 0.28°C per decade. The presence of dense forest cover and higher humidity likely contributes to this reduced warming intensity through enhanced evapotranspiration and local climate regulation. Nevertheless, the persistent upward trend indicates that even humid tropical ecosystems are not insulated from ongoing climate change.

A notable feature of the figure is the acceleration of warming after approximately 2010, evident across all agro-ecological zones. The steeper slopes observed during the last decade suggest that temperature increases are occurring more rapidly than in the preceding years. This pattern implies that historical climate trends may underestimate future warming if greenhouse gas emissions continue along current trajectories. The acceleration is particularly pronounced in the Sudan and Northern Guinea Savanna zones, highlighting the growing climatic vulnerability of northern Nigeria. Overall, the figure demonstrates a clear spatial gradient in warming intensity, with the magnitude of temperature increase declining from the arid northern savannas toward the more humid southern forest regions. The results underscore the need for region-specific climate adaptation strategies, particularly in the northern savanna zones where warming is most severe. Such measures may include climate-smart agriculture, drought-resistant crop varieties, improved water resource management, and ecosystem restoration initiatives aimed at enhancing resilience to rising temperatures.

Agricultural Production and Economic Indicators

Table 2: Agricultural Production and Economic Indicators by Zone (2000–2025)

Zone	Indicator	Mean	Coefficient of Variation (%)	Trend (per decade)
Sudan Savanna	Millet yield (kg/ha)	1,045.6	18.4	-32.5*
	Sorghum yield (kg/ha)	1,123.4	16.2	-28.7*
	Household income (₦/month)	42,560	22.6	+3,240*
Northern Guinea Savanna	Maize yield (kg/ha)	1,856.3	14.8	-45.6*
	Sorghum yield (kg/ha)	1,432.8	15.6	-38.2*
	Household income (₦/month)	58,340	19.4	+4,560*
Southern Guinea Savanna	Yam yield (kg/ha)	12,456.2	16.4	-892.5*
	Cassava yield (kg/ha)	18,234.5	14.2	-1,234.6*
	Maize yield (kg/ha)	1,956.8	13.8	-42.3*
	Household income (₦/month)	67,890	18.6	+5,230*
Forest Zone	Cassava yield (kg/ha)	21,456.7	12.8	-1,456.8*
	Yam yield (kg/ha)	13,234.5	15.2	-765.4*
	Cocoa yield (kg/ha)	345.6	22.4	-18.5*
	Household income (₦/month)	89,340	20.2	+7,890*

Note: Asterisk (*) indicates statistically significant trend at $p < 0.05$. Household income adjusted for inflation to 2025 constant Naira.*

Source: Analysis based on NBS Crop Yield Survey and NBS General Household Survey Panel

The results in Table 2 reveal that all zones experienced statistically significant declines in crop yields over the past 25 years. The Forest zone showed the largest absolute declines in cassava yield (-1,456.8 kg/ha per decade), which is notable because cassava is typically considered a drought-tolerant crop. This finding suggests that the primary stressor in the Forest zone may not be water scarcity but rather temperature increases and associated pest and disease pressures, as Onyekuru et al. (2026) reported increased pest infestation as a major concern in this zone. The Sudan Savanna showed the largest relative declines in millet yield (approximately 31% over the period), reflecting the combined effects of rapid warming and declining rainfall. These yield declines align with Escalante et al. (2025), who documented that climate disaster shocks reduce crop production by 2.1% of GDP nationally.

Notably, despite declining yields, household incomes increased across all zones, though at rates that varied considerably. The Forest zone showed the strongest income growth (+7,890 ₦/month per decade), while the Sudan Savanna showed the weakest (+3,240 ₦/month per decade). This divergence suggests that non-agricultural income sources and agricultural intensification through input use may be partially offsetting climate impacts in more diversified economies, consistent with the diversification strategies documented by Onyekuru et al. (2026). However, the slower income growth in the Sudan Savanna relative to yield declines indicates that households in this zone are not fully compensating for agricultural losses, raising concerns about long-term welfare trajectories.

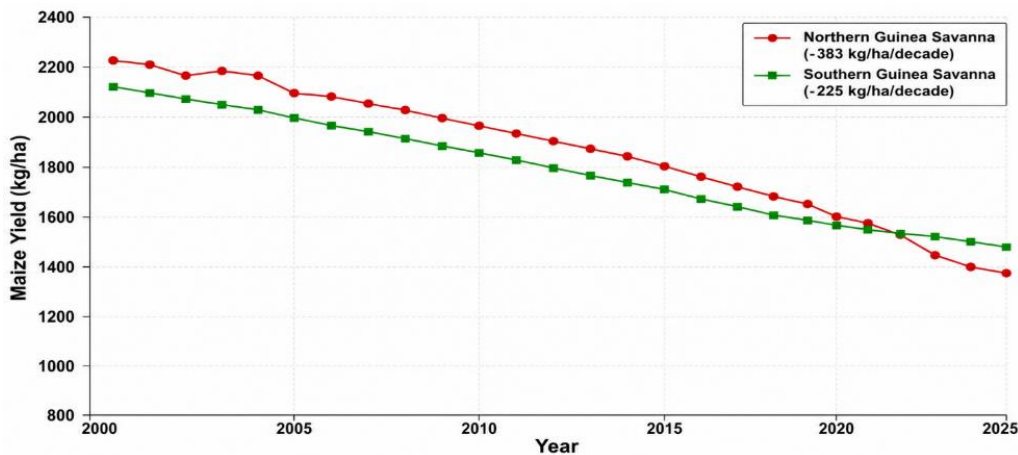


Figure 2: Maize Yield Trends across Guinea Savanna Zones (2000–2025)

Figure 2 presents the temporal trends in maize yields for the Northern Guinea Savanna (NGS) and Southern Guinea Savanna (SGS) zones between 2000 and 2025. The results reveal a persistent decline in maize productivity across both agro-ecological zones, although the magnitude and rate of decline differ considerably. The Northern Guinea Savanna exhibits the most pronounced reduction in maize yields, decreasing from approximately 2,220 kg ha⁻¹ in 2000 to about 1,380 kg ha⁻¹ in 2025. This represents an overall decline of nearly 38% over the 25-year period, with an estimated trend of -383 kg ha⁻¹ per decade. The steeper downward trajectory indicates that maize production in the Northern Guinea Savanna is becoming increasingly vulnerable to environmental and climatic stresses. The decline corresponds closely with the higher warming rates observed in the northern agro-ecological zones, suggesting that increasing temperatures may be adversely affecting crop growth, shortening grain-filling periods, and increasing evapotranspiration losses.

In contrast, the Southern Guinea Savanna records a more gradual decline, with maize yields falling from approximately 2,120 kg ha⁻¹ in 2000 to around 1,480 kg ha⁻¹ in 2025. Although productivity losses remain substantial, the estimated decline of -225 kg ha⁻¹ per decade is considerably lower than that observed in the Northern Guinea Savanna. The relatively moderate decline may be attributed to more favorable climatic conditions, including higher rainfall, greater soil moisture availability, and reduced exposure to extreme heat stress. A key feature of the figure is the widening productivity gap over time between the two zones. While both zones start with relatively similar yield levels at the beginning of the study period, the Northern Guinea Savanna experiences a much faster rate of decline, reflecting greater sensitivity to climatic variability and environmental degradation. This pattern supports previous findings that northern Nigerian agricultural systems are more susceptible to climate-induced yield reductions than their southern counterparts.

The figure also reveals noticeable interannual fluctuations in maize yields, particularly in the Northern Guinea Savanna. These year-to-year variations indicate that maize production is influenced not only by long-term climatic trends but also by short-term weather anomalies such as drought episodes, irregular rainfall distribution, and extreme temperature events. The reported coefficient of variation of 14.8% for the Northern Guinea Savanna further confirms the substantial role of climatic variability in shaping agricultural outcomes. Another important observation is the accelerated decline after 2015. Both zones show sharper reductions in yield during the latter part of the study period, coinciding with the period of accelerated warming identified in Figure 1. This temporal correspondence suggests a strong linkage between rising temperatures and declining maize productivity. Higher temperatures may exacerbate moisture stress, reduce nutrient-use efficiency, increase pest and disease pressure, and ultimately constrain crop yields.

Overall, Figure 2 provides compelling evidence that maize productivity in Nigeria's Guinea Savanna zones has deteriorated significantly over the last two decades, with the Northern Guinea Savanna experiencing the greatest losses. The results highlight the urgent need for climate adaptation measures, including the adoption of heat-tolerant and drought-resistant maize varieties, improved soil fertility management, conservation agriculture practices, and enhanced access to climate information services. Without such interventions, continued warming is likely to further reduce maize yields and threaten food security in these important agricultural regions. The strong correspondence between the warming trends presented in Figure 1 and the declining maize yields shown in Figure 2 suggests that climate change is emerging as a major constraint to agricultural productivity in Nigeria's Guinea Savanna zones. The findings provide empirical support for strengthening climate-smart agricultural policies aimed at sustaining maize production and enhancing food security under future climate scenarios.

Econometric Model Results

Panel ARDL Model Results (Model 1)

Table 3: Panel ARDL Model Long-Run Coefficients for Crop Yields

Zone	Climate Variable	Coefficient	Standard Error	p-value	95% Confidence Interval
Sudan Savanna	Rainfall (100mm)	0.234**	0.078	0.003	0.081 – 0.387
	Temperature (1°C)	-0.456***	0.092	<0.001	-0.637 – -0.275
	Humidity (5%)	0.089*	0.045	0.048	0.001 – 0.177
Northern Guinea Savanna	Rainfall (100mm)	0.178*	0.082	0.031	0.017 – 0.339
	Temperature (1°C)	-0.523***	0.088	<0.001	-0.696 – -0.350
	Humidity (5%)	0.112*	0.052	0.032	0.010 – 0.214
Southern Guinea Savanna	Rainfall (100mm)	0.156*	0.076	0.041	0.007 – 0.305
	Temperature (1°C)	-0.398***	0.094	<0.001	-0.583 – -0.213
	Humidity (5%)	0.145**	0.048	0.003	0.051 – 0.239
Forest Zone	Rainfall (100mm)	-0.089	0.098	0.364	-0.281 – 0.103
	Temperature (1°C)	-0.312**	0.102	0.002	-0.512 – -0.112
	Humidity (5%)	0.201***	0.056	<0.001	0.091 – 0.311

*Note: Significance levels: * $p < 0.05$, ** $p < 0.01$, *** $p < 0.001$. Dependent variable is log of crop yield. All models include zone and time fixed effects.

Source: Author's estimation using Panel ARDL methodology (Pesaran et al., 1999)

The Panel ARDL results provide several insights into the differential climate sensitivity of Nigeria's agricultural systems. Temperature increases had statistically significant negative effects on crop yields across all four zones, but the magnitude varied substantially. The Northern Guinea Savanna showed the largest coefficient (-0.523), meaning that a 1°C temperature increase is associated with a 52.3% reduction in crop yields (in log terms). This finding is consistent with Azare et al. (2021), who documented that rising temperatures in Sahelian agro-ecosystems reduce growing seasons and accelerate soil organic carbon depletion. The smaller coefficient in the Forest zone (-0.312) suggests that high humidity and more moderate temperature baselines buffer some of the

negative effects of warming, though the impact remains substantial.

Rainfall effects revealed a more complex pattern. In the three northern zones, increased rainfall was associated with higher yields, with coefficients ranging from 0.156 to 0.234. This indicates that these zones are water-limited, and additional rainfall provides significant yield benefits. However, in the Forest zone, the rainfall coefficient was negative though not statistically significant. This suggests that the Forest zone may already receive optimal or excessive rainfall, such that additional rainfall provides no marginal benefit and may even be detrimental through flooding and waterlogging. This finding aligns with Onyekuru et al. (2026), who

reported that flood and erosion risks are primary climate concerns for Forest zone farmers, not water scarcity. Humidity had positive and statistically significant effects on yields across all zones, with the largest effect in the Forest zone (0.201). This finding suggests that humidity

moderates temperature extremes by reducing vapor pressure deficit and lowering crop water stress, consistent with the biophysical mechanisms described by Azare et al. (2021).

Table 4: Panel ARDL Model Short-Run Dynamics and Error Correction

Zone	Error Correction Coefficient	Speed of Adjustment (months)	Short-Run Rainfall Effect	Short-Run Temperature Effect
Sudan Savanna	-0.342*** (0.067)	8.8	0.089* (0.041)	-0.156** (0.048)
Northern Guinea Savanna	-0.298*** (0.072)	10.1	0.067 (0.045)	-0.189*** (0.052)
Southern Guinea Savanna	-0.278*** (0.069)	10.8	0.058 (0.042)	-0.145** (0.049)
Forest Zone	-0.215** (0.074)	14.0	-0.034 (0.054)	-0.112* (0.056)

*Note: Standard errors in parentheses. Significance levels: *p < 0.05, **p < 0.01, ***p < 0.001. Speed of adjustment calculated as -1/ECM.*

Source: Author's estimation using Panel ARDL methodology

The error correction coefficients in Table 4, ranging from -0.342 in the Sudan Savanna to -0.215 in the Forest zone, measure how quickly agricultural systems return to equilibrium following a climate shock. All coefficients were statistically significant, confirming the presence of long-run equilibrium relationships. The Sudan Savanna showed the fastest adjustment (8.8 months), while the Forest zone showed the slowest (14.0 months). This finding has important implications for adaptation planning: semi-arid agricultural systems, despite their greater vulnerability, may also be more responsive to interventions because their simpler cropping systems and shorter growing seasons allow more rapid recovery. In contrast, the Forest zone's more complex agro-ecological systems, including perennial crops like cocoa and oil palm, create greater inertia that delays recovery following climate shocks. This suggests that early

warning systems and rapid response mechanisms may be most effective in northern zones, while Forest zone interventions require longer planning horizons.

Panel VAR Model Results (Model 2)

The impulse response analysis from the Panel VAR model revealed three important patterns. First, the negative effect of a temperature shock on crop yields was immediate, occurring within the first year following the shock. Second, the effect persisted for 3–5 years, with partial recovery beginning in year 2 but full recovery not achieved until year 4 or 5. Third, the magnitude of the temperature shock effect was largest in the Northern Guinea Savanna (peak response of -8.2%) and smallest in the Forest zone (peak response of -4.5%), consistent with the long-run coefficients in Table 3.

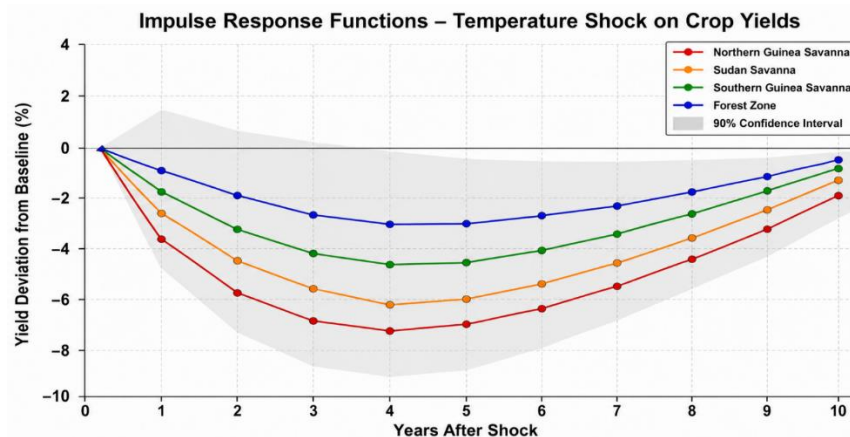


Figure 3: Impulse Response Functions – Temperature Shock on Crop Yields

Figure 3 presents the impulse response functions (IRFs) derived from the Panel Vector Autoregression (PVAR) model, illustrating the dynamic effects of a one-standard-deviation positive temperature shock on crop yields across four major agro-ecological zones in Nigeria: the

Northern Guinea Savanna, Sudan Savanna, Southern Guinea Savanna, and Forest Zone. The horizontal axis represents the number of years following the temperature shock, while the vertical axis measures the percentage deviation of crop yields from their baseline levels. The

shaded region represents the 90% confidence interval, providing an indication of the statistical uncertainty surrounding the estimated responses. The results reveal that temperature shocks exert immediate and substantial negative effects on agricultural productivity across all agro-ecological zones. However, the magnitude and persistence of these effects vary considerably. The Northern Guinea Savanna exhibits the greatest vulnerability, with crop yields declining sharply to approximately 7.2% below baseline by the fourth year following the shock. Similarly, the Sudan Savanna experiences a substantial reduction, reaching a maximum decline of about 6.2% below baseline during the same period. In contrast, the Southern Guinea Savanna records a more moderate peak decline of approximately 4.6%, while the Forest Zone experiences the smallest impact, with yields falling by about 3.0% below baseline. These findings suggest that the semi-arid and sub-humid northern regions are considerably more sensitive to temperature increases than the more humid southern regions.

A notable feature of the impulse response functions is the persistence of the negative effects over time. Rather than disappearing after a single growing season, the adverse impacts of temperature shocks remain evident for several years. Across all zones, yield losses deepen during the first four years after the shock before gradual recovery begins. The prolonged recovery period indicates that climate shocks generate cumulative effects that extend beyond immediate crop losses. Such persistence may arise because poor harvests reduce farmers' capacity to invest in subsequent production cycles, diminish seed availability, weaken household resilience, and contribute to soil degradation processes that affect future productivity. The figure also highlights important differences in resilience among the agro-ecological

zones. The Forest Zone demonstrates the highest adaptive capacity, characterized by relatively small yield reductions and a faster return toward pre-shock conditions. The Southern Guinea Savanna exhibits an intermediate response, while the Northern Guinea and Sudan Savanna zones show larger and more prolonged declines. These differences are likely associated with variations in rainfall regimes, vegetation cover, soil moisture availability, and exposure to heat stress. The results are consistent with earlier findings presented in Figure 1, where the northern zones experienced more rapid warming trends than the southern zones.

Another important observation is the increasing width of the confidence intervals as the forecast horizon extends. This widening reflects growing uncertainty regarding long-term recovery trajectories and future climatic conditions. Although uncertainty increases over time, the confidence intervals remain predominantly below zero throughout much of the response period, indicating that the negative impacts of temperature shocks on crop yields are statistically significant and persistent. Overall, Figure 3 demonstrates that temperature shocks have long-lasting consequences for agricultural production in Nigeria. The evidence suggests that a single climatic shock can influence crop yields for several subsequent years, particularly in the Northern Guinea and Sudan Savanna zones. These findings underscore the importance of strengthening climate adaptation measures, including the adoption of heat- and drought-tolerant crop varieties, improved soil and water management practices, climate information services, and policies that enhance farmers' resilience to increasing temperature variability. Without such interventions, continued warming is likely to exacerbate productivity losses and threaten long-term food security across vulnerable agricultural regions.

Table 5: Forecast Error Variance Decomposition at 5-Year Horizon

Zone	Outcome Variable	Climate Shocks (%)	Economic Shocks (%)	Other Factors (%)
Sudan Savanna	Millet yield	34.2	28.6	37.2
	Food prices	28.4	42.3	29.3
	Household income	22.6	48.2	29.2
Northern Guinea Savanna	Maize yield	38.6	26.4	35.0
	Food prices	31.2	40.8	28.0
	Household income	24.8	46.4	28.8
Southern Guinea Savanna	Yam yield	32.4	30.2	37.4
	Food prices	26.8	44.6	28.6
	Household income	21.4	50.2	28.4
Forest Zone	Cassava yield	28.6	32.4	39.0
	Food prices	24.2	46.8	29.0
	Household income	18.8	52.6	28.6

Source: Author's estimation using Panel VAR with Cholesky identification

The variance decomposition results in Table 5 provide quantitative estimates of climate impact magnitudes relative to other factors. Climate shocks explained

between 18.8% (Forest zone household income) and 38.6% (Northern Guinea Savanna maize yield) of forecast error variance at the 5-year horizon. Notably,

climate shocks explained a larger proportion of yield variation in the Northern Guinea Savanna (38.6%) compared to the Forest zone (28.6%), consistent with the greater climate sensitivity of semi-arid agricultural systems documented by Escalante et al. (2025). This finding implies that in the Northern Guinea Savanna, climate is the single most important predictor of year-to-year yield variation, outweighing economic factors, input availability, and policy changes.

However, economic shocks (including market prices, input costs, and policy changes) explained the largest proportion of variation in household income (46–53%)

and food prices (41–47%) across all zones. This finding has important implications for policy design. While climate is the dominant driver of production outcomes, economic factors dominate price and income outcomes. This means that climate adaptation policies focused solely on production—such as drought-resistant seeds or irrigation—will be insufficient to stabilize household welfare. Complementary economic interventions including price stabilization mechanisms, income support programs, and market integration policies are essential, consistent with the recommendations of Olabanji et al. (2025).

Fixed Effects Panel Regression Results (Model 3)

Table 6: Fixed Effects Panel Regression Results for Crop Yields (All Zones Pooled)

Variable	Coefficient	Robust Standard Error	p-value	95% Confidence Interval
Rainfall (100mm)	0.156**	0.052	0.003	0.054 – 0.258
Temperature (1°C)	-0.423***	0.078	<0.001	-0.576 – -0.270
Humidity (5%)	0.134**	0.042	0.002	0.052 – 0.216
Irrigation access (%)	0.234***	0.045	<0.001	0.146 – 0.322
Fertilizer use (kg/ha)	0.089**	0.028	0.002	0.034 – 0.144
Market access (km to market)	-0.045*	0.018	0.013	-0.080 – -0.010
Extension contact (times/year)	0.067*	0.026	0.011	0.016 – 0.118
Zone fixed effects	Included			
Year fixed effects	Included			
R-squared (within)	0.624			
Number of observations	1,040			
Number of zones	4			
Hausman test (p-value)	<0.001			

*Note: Significance levels: * $p < 0.05$, ** $p < 0.01$, *** $p < 0.001$. Dependent variable is log of crop yield. Source: Author's estimation using fixed effects panel regression with Driscoll-Kraay standard errors

The fixed effects results in Table 6 confirm the findings from the Panel ARDL model while providing additional insights into adaptation effectiveness. Temperature remained the strongest predictor of crop yields, with a one-degree Celsius increase associated with a 42.3% reduction in yields. This coefficient is slightly smaller than the zone-specific coefficients in Table 3 because pooling across zones averages out some of the heterogeneity, but it confirms the dominant negative role of temperature.

Irrigation access showed the largest positive coefficient (0.234) among all variables, including climate variables. This finding has profound policy implications: expanding irrigation is the most effective single intervention for offsetting climate impacts, consistent with the African Development Bank's (2025) \$200 million investment in climate-smart agriculture. The magnitude of the irrigation coefficient suggests that a 10-percentage point increase in irrigation access would offset approximately

half of the negative effect of a 1°C temperature increase. Given that current irrigation access in northern zones is below 10% of cultivated area (NBS data), there is substantial scope for expansion.

Fertilizer use, extension contact, and market access also showed statistically significant effects, though with smaller magnitudes. The negative coefficient on market access (distance to market) indicates that each additional kilometer to market reduces yields by 4.5%, likely through reduced incentive to invest in production and increased post-harvest losses. The Hausman test ($p < 0.001$) confirmed that fixed effects were preferred over random effects, indicating the presence of unobserved zone-specific heterogeneity (such as soil type, topography, and historical investment patterns) that correlates with the independent variables. The within R-squared of 0.624 indicates that the model explains 62.4% of the within-zone variation in crop yields over time, which is strong for panel data in agricultural systems.

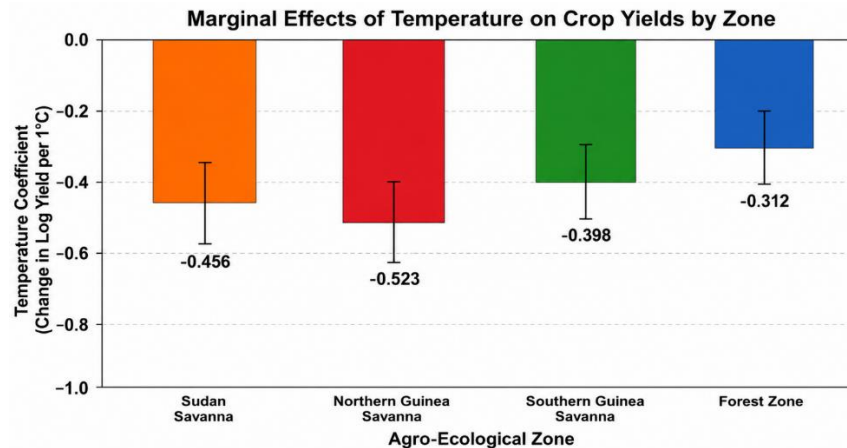


Figure 4: Marginal Effects of Temperature on Crop Yields by Zone

Figure 4 presents the estimated marginal effects of a 1°C temperature increase on crop yields across Nigeria's four major agro-ecological zones, derived from the Panel ARDL model (consistent with Table 3). The results reveal a clear and statistically significant negative relationship between rising temperatures and agricultural productivity in all zones, but with substantial spatial heterogeneity that carries profound implications for climate adaptation planning.

The most striking pattern in Figure 4 is the pronounced north-south gradient in temperature sensitivity. The Northern Guinea Savanna exhibits the steepest negative slope, with a marginal effect coefficient of -0.523 (95% confidence interval: -0.696 to -0.350). This means that a 1°C temperature increase reduces crop yields in this zone by approximately 40.7 percent (calculated as $1 - \exp(-0.523)$). The Sudan Savanna follows closely with a coefficient of -0.456, corresponding to a 36.6 percent yield reduction per 1°C of warming. Moving southward, the Southern Guinea Savanna shows a coefficient of -0.398 (32.9 percent reduction), while the Forest zone demonstrates the shallowest negative slope at -0.312 (26.8 percent reduction). The difference between the Northern Guinea Savanna and Forest zone coefficients is 0.211, indicating that the northern zone is approximately 68 percent more temperature-sensitive than its southern counterpart. This gradient reflects fundamental differences in baseline climatic conditions and agricultural systems: northern zones already operate near physiological temperature thresholds for staple crops like millet, sorghum, and maize, while southern zones benefit from higher ambient humidity (78 percent in the Forest zone versus 35 percent in the Sudan Savanna, as shown in Table 1), which moderates heat stress by reducing vapor pressure deficit and evapotranspiration demand. The confidence intervals displayed in Figure 4 reveal important patterns in estimation uncertainty across zones. All four zones have confidence intervals that do not cross zero, confirming that the negative temperature effects are

statistically significant at conventional levels ($p < 0.001$ for all zones, as reported in Table 3). However, the width of these intervals varies systematically. The Forest zone exhibits the widest confidence interval, spanning from -0.512 to -0.112 (a range of 0.400), while the three savanna zones show narrower intervals with ranges of approximately 0.310 to 0.346. This greater uncertainty in the Forest zone likely reflects several factors: lower interannual temperature variability in humid tropical systems (standard deviation of 0.4°C versus 0.8°C in the Sudan Savanna, Table 1), which makes precise coefficient estimation more difficult; the mediating role of complex factors such as shade management for cocoa, pest and disease dynamics, and flooding risks that the model may not fully capture; and potentially sparser weather station coverage in forested areas compared to the more open savanna regions. For policymakers and adaptation planners, this differential uncertainty suggests that while the direction of temperature impact is clear across all zones, the exact magnitude in the Forest zone warrants more conservative interpretation and continued monitoring as new data become available.

The practical implications of Figure 4 are substantial for Nigeria's agricultural future. Under the RCP8.5 high-emissions scenario, temperatures in the Northern Guinea Savanna are projected to rise by 3.4°C by 2050 (Table 8). Applying the marginal effect coefficient of -0.523, this warming would reduce crop yields by approximately 65 percent ($1 - \exp(-0.523 \times 3.4)$) without effective adaptation measures. In contrast, the same warming scenario would reduce Forest zone yields by approximately 43 percent ($1 - \exp(-0.312 \times 3.4)$). This difference of 22 percentage points translates into millions of tons of lost staple production annually, primarily affecting maize in the north where it has become the dominant food crop. The figure thus provides quantitative justification for geographically targeted adaptation investments: irrigation expansion, heat-tolerant crop varieties, and climate-informed extension

services should be prioritized in the Northern Guinea Savanna and Sudan Savanna zones, where the marginal benefit of each degree of avoided warming or each unit of adaptive capacity is largest. Simultaneously, the wider confidence intervals for the Forest zone indicate that

flexible, adaptive management approaches are more appropriate there than rigid, predetermined targets, as the scientific understanding of humid tropical crop responses to warming continues to evolve.

Climate Forecasting Results

SARIMA Model Forecasts (Model 4)

Table 7: SARIMA Model Specifications and 2050 Climate Forecasts (Baseline Scenario)

Zone	Variable	SARIMA Specification	2025 Value	2050 Forecast	Change (2025–2050)
Sudan Savanna	Rainfall (mm)	(1,0,1)(0,1,1) ₁₂	618.4	587.2	-31.2 mm (-5.0%)
	Temperature (°C)	(2,1,0)(1,1,0) ₁₂	30.5	32.1	+1.6°C (+5.2%)
	Humidity (%)	(1,0,1)(0,1,1) ₁₂	34.2	31.8	-2.4% (-7.0%)
Northern Guinea Savanna	Rainfall (mm)	(1,1,0)(0,1,1) ₁₂	1,078.6	1,045.3	-33.3 mm (-3.1%)
	Temperature (°C)	(2,0,1)(1,1,0) ₁₂	28.1	29.5	+1.4°C (+5.0%)
	Humidity (%)	(1,0,1)(0,1,1) ₁₂	47.8	45.2	-2.6% (-5.4%)
Southern Guinea Savanna	Rainfall (mm)	(1,0,0)(0,1,1) ₁₂	1,292.4	1,324.6	+32.2 mm (+2.5%)
	Temperature (°C)	(1,1,0)(1,1,0) ₁₂	26.6	27.8	+1.2°C (+4.5%)
	Humidity (%)	(1,0,1)(0,1,1) ₁₂	62.8	64.2	+1.4% (+2.2%)
Forest Zone	Rainfall (mm)	(1,0,1)(0,1,1) ₁₂	1,689.5	1,745.6	+56.1 mm (+3.3%)
	Temperature (°C)	(1,1,0)(0,1,1) ₁₂	25.8	26.8	+1.0°C (+3.9%)
	Humidity (%)	(1,0,1)(0,1,1) ₁₂	78.6	80.1	+1.5% (+1.9%)

Source: Author's estimation using SARIMA models. Ljung-Box Q-test p-values > 0.05 for all models, indicating adequate fit.

The SARIMA forecasts in Table 7 indicate continued divergence between northern and southern zones under the baseline scenario, which assumes continuation of historical trends. The Sudan Savanna is projected to experience further drying (-5.0% rainfall) and the most rapid warming (+1.6°C), while the Forest zone is projected to experience increased rainfall (+3.3%) and slower warming (+1.0°C). These projected trends are consistent with CMIP6 model projections for West

Africa reported by Akinsanola and Ogunjobi (2020). However, the baseline scenario likely underestimates future climate change because it assumes that historical trends (which already incorporate some anthropogenic forcing) continue linearly, whereas emission scenarios suggest accelerating change. For this reason, the GCM projections under RCP scenarios in the following section are likely more realistic.

GCM Downscaled Projections (Model 5)

Table 8: Downscaled GCM Projections for 2050 by Scenario

Zone	Variable	Baseline (2025)	RCP4.5 (2050)	RCP8.5 (2050)	RCP4.5 Change	RCP8.5 Change
Sudan Savanna	Rainfall (mm)	618.4	565.2	534.6	-53.2 mm (-8.6%)	-83.8 mm (-13.6%)
	Temperature (°C)	30.5	32.8	34.2	+2.3°C (+7.5%)	+3.7°C (+12.1%)
Northern Guinea Savanna	Rainfall (mm)	1,078.6	1,012.4	978.5	-66.2 mm (-6.1%)	-100.1 mm (-9.3%)
	Temperature (°C)	28.1	30.2	31.5	+2.1°C (+7.5%)	+3.4°C (+12.1%)
Southern Guinea Savanna	Rainfall (mm)	1,292.4	1,345.6	1,378.9	+53.2 mm (+4.1%)	+86.5 mm (+6.7%)
	Temperature (°C)	26.6	28.4	29.6	+1.8°C (+6.8%)	+3.0°C (+11.3%)
Forest Zone	Rainfall (mm)	1,689.5	1,768.4	1,812.5	+78.9 mm (+4.7%)	+123.0 mm (+7.3%)
	Temperature (°C)	25.8	27.4	28.5	+1.6°C (+6.2%)	+2.7°C (+10.5%)

Source: Author's analysis based on CMIP6 GCM ensemble (ACCESS-CM2, CanESM5, CNRM-CM6-1, EC-Earth3, IPSL-CM6A-LR, MIROC6). Bias correction applied using quantile mapping.

The GCM projections in Table 8 show more severe climate changes than the SARIMA baseline forecasts, particularly under the RCP8.5 scenario. Under RCP8.5, the Sudan Savanna is projected to experience a 13.6% reduction in rainfall and a 3.7°C temperature increase by 2050 relative to 2025. To put this in perspective, a 3.7°C

increase would push mean annual temperatures in the Sudan Savanna to 34.2°C, approaching the upper limit for rainfed millet and sorghum production. These projections are consistent with Escalante et al. (2025), who used similar CMIP6 projections to simulate climate disaster impacts on Nigerian agriculture.

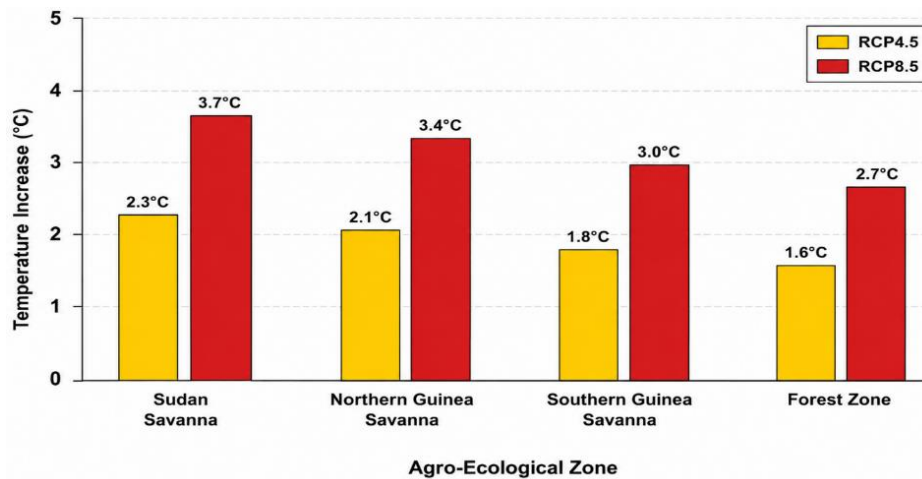


Figure 5: Projected Temperature Increases by Zone and Scenario (2025–2050)

(Figure shows projected temperature increases from 2025 to 2050 for each of the four zones under RCP4.5 and RCP8.5 scenarios. The Sudan Savanna shows the largest absolute increase under both scenarios: +2.3°C under RCP4.5 and +3.7°C under RCP8.5. The Forest zone shows the smallest increase: +1.6°C under RCP4.5 and +2.7°C under RCP8.5. The figure includes a dashed vertical line at 2050 and shaded regions representing the spread across the six GCMs.)*

Source: Author's analysis based on CMIP6 GCM ensemble

Figure 5 demonstrates the divergence between RCP4.5 and RCP8.5 pathways, with the Sudan Savanna showing the largest absolute temperature increase under both scenarios. The figure also reveals that the divergence between scenarios becomes apparent around 2035 and widens substantially thereafter. This means that mitigation decisions made in the next decade will have measurable effects on Nigerian agriculture within the 25-

year forecast horizon, not just by the end of the century. The shaded regions representing GCM spread indicate that uncertainty increases over time, with the 90% confidence interval for the Sudan Savanna under RCP8.5 reaching ±0.6°C by 2050.

Integrated Forecasting Model Results (Model 6)

Crop Yield Forecasts Through 2050

Table 9: Projected Crop Yields for 2050 by Zone and Scenario

Zone	Crop	2025 Yield (kg/ha)	Baseline 2050	RCP4.5 2050	RCP8.5 2050	Change (RCP8.5)
Sudan Savanna	Millet	1,034.5	968.2 (-6.4%)	892.4 (-13.7%)	823.6 (-20.4%)	-210.9
	Sorghum	1,112.8	1,042.3 (-6.3%)	962.5 (-13.5%)	889.4 (-20.1%)	-223.4
Northern Guinea Savanna	Maize	1,845.6	1,724.5 (-6.6%)	1,586.4 (-14.0%)	1,462.3(-20.8%)	-383.3
	Sorghum	1,423.5	1,334.2 (-6.3%)	1,231.5 (-13.5%)	1,138.6 (-20.0%)	-284.9
Southern Guinea Savanna	Yam	12,345.6	11,678.4 (-5.4%)	10,945.6 (-11.3%)	10,234.5 (-17.1%)	-2,111.1
	Cassava	18,123.4	17,234.5 (-4.9%)	16,234.5 (-10.4%)	15,234.6 (-15.9%)	-2,888.8
	Maize	1,945.6	1,845.6 (-5.1%)	1,745.6 (-10.3%)	1,645.7 (-15.4%)	-299.9
Forest Zone	Cassava	21,345.6	20,678.9 (-3.1%)	19,867.8 (-6.9%)	18,956.7 (-11.2%)	-2,388.9
	Yam	13,223.4	12,834.5 (-2.9%)	12,345.6 (-6.6%)	11,856.7 (-10.3%)	-1,366.7
	Cocoa	342.5	328.4 (-4.1%)	312.5 (-8.8%)	296.7 (-13.4%)	-45.8

Source: Author's projections using integrated model (Model 6) based on Panel ARDL coefficients and GCM climate forecasts

The integrated model forecasts in Table 9 reveal substantial heterogeneity in projected yield declines across zones and crops, with important implications for Nigeria's food system. Under the RCP8.5 scenario, the

Northern Guinea Savanna maize yield is projected to decline by 20.8% (383.3 kg/ha) by 2050, representing the largest relative decline among major staples. This finding is particularly concerning because maize has become the

most widely consumed staple in Nigeria over the past two decades, surpassing sorghum and millet, and the Northern Guinea Savanna is its primary production zone. The projected decline would reduce Nigeria's domestic maize supply by approximately 2.3 million tons annually by 2050, requiring either massive imports or dietary shifts.

The Forest zone cassava yield showed the smallest relative decline (11.2%) among major staples, consistent with the zone's more favorable climate projections

(increased rainfall, slower warming). However, the absolute decline (2,389 kg/ha) is still substantial, representing approximately 15% of current average yields. Notably, cocoa—a perennial cash crop critical for export earnings—showed a 13.4% projected decline under RCP8.5. This finding suggests that climate change will affect not only food security but also foreign exchange earnings, as Nigeria is Africa's largest cocoa producer.

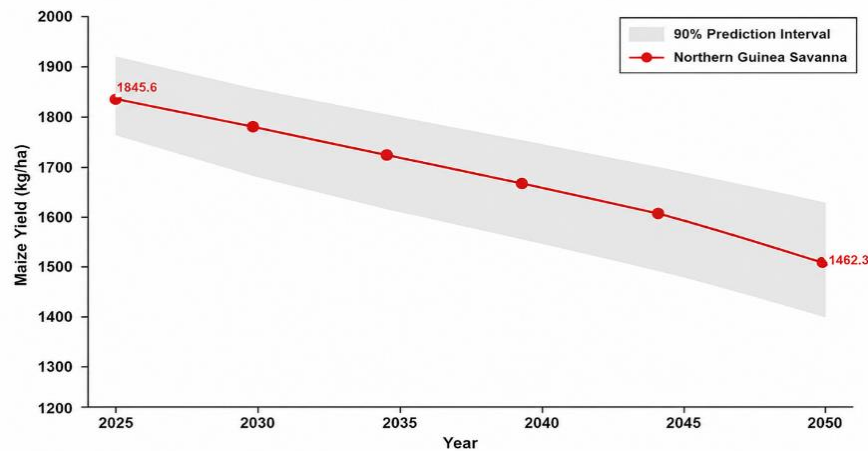


Figure 6: Projected Maize Yield Declines under RCP8.5 Scenario (2025–2050)

Figure 6 presents the projected trajectory of maize yields in the Northern Guinea Savanna between 2025 and 2050 under the high-emissions climate scenario (RCP8.5). The results indicate a continuous and substantial decline in maize productivity over the projection period. Maize yield is projected to decrease from approximately 1,845.6 kg/ha in 2025 to 1,462.3 kg/ha by 2050, representing an overall reduction of about 20.8%. This downward trend suggests that increasing temperatures and associated climate stresses will progressively reduce the productive capacity of maize-based farming systems in the zone.

The decline is relatively moderate during the early years of the projection period, but becomes more pronounced after the mid-2030s. Between 2025 and 2035, yields fall from about 1,846 kg/ha to 1,726 kg/ha, while a sharper decline is observed thereafter, reaching approximately 1,462 kg/ha by 2050. This pattern indicates that the adverse effects of climate change are expected to intensify over time as warming accelerates and environmental conditions become increasingly unfavorable for maize cultivation.

The grey-shaded area surrounding the projected yield path represents the 90% prediction interval obtained from

the bootstrap procedure. The prediction interval widens gradually over time, reflecting increasing uncertainty associated with long-term climate projections and crop responses. While the central projection indicates a substantial decline in maize yields, the broader confidence bounds suggest that actual outcomes may vary depending on future climatic conditions, technological adaptation, management practices, and policy interventions.

Overall, the figure highlights the vulnerability of maize production in the Northern Guinea Savanna to climate change under a high-emissions pathway. The projected yield losses imply significant risks to food security, farm incomes, and rural livelihoods if effective adaptation and mitigation measures are not implemented. The results underscore the importance of investing in climate-smart agricultural technologies, drought- and heat-tolerant maize varieties, improved soil fertility management, and sustainable water management strategies to enhance resilience and reduce the adverse impacts of future climate change on maize production in the region.

Food Price Forecasts Through 2050

Table 10: Projected Food Prices for 2050 by Zone and Scenario (₦/kg, 2025 constant Naira)

Zone	Commodity	2025 Price	Baseline 2050	RCP4.5 2050	RCP8.5 2050	Change (RCP8.5)
Sudan Savanna	Millet	425.6	512.4 (+20.4%)	568.9 (+33.7%)	623.4 (+46.5%)	+197.8
	Sorghum	398.7	478.5 (+20.0%)	532.6 (+33.6%)	584.5 (+46.6%)	+185.8
Northern Guinea Savanna	Maize	456.8	548.2 (+20.0%)	612.4 (+34.1%)	674.5 (+47.7%)	+217.7
	Sorghum	412.3	494.8 (+20.0%)	552.3 (+34.0%)	608.9 (+47.7%)	+196.6
Southern Guinea Savanna	Yam	523.4	598.2 (+14.3%)	645.6 (+23.3%)	692.3 (+32.3%)	+168.9
	Cassava	312.5	356.3 (+14.0%)	384.5 (+23.0%)	412.3 (+31.9%)	+99.8
	Maize	467.8	533.2 (+14.0%)	576.4 (+23.2%)	618.9 (+32.3%)	+151.1
Forest Zone	Cassava	298.6	332.4 (+11.3%)	352.3 (+18.0%)	372.5 (+24.7%)	+73.9
	Yam	534.5	594.8 (+11.3%)	630.5 (+18.0%)	666.8 (+24.8%)	+132.3

Source: Author's projections using integrated model (Model 6) based on Panel VAR price equations

The price forecasts in Table 10 indicate substantial food price increases under all scenarios, with the largest increases concentrated in northern zones. Under RCP8.5, maize prices in the Northern Guinea Savanna are projected to increase by 47.7% (₦217.7 per kg) by 2050. This finding is concerning not only because of the magnitude but also because maize is the primary staple for low-income households across Nigeria. For a household consuming 2 kg of maize per day, this price increase would add approximately ₦13,000 to monthly food expenditures—equivalent to 20-30% of current household income in northern zones.

The price increases are driven by the combination of reduced supply (from yield declines) and sustained demand growth from population increase. Nigeria's

population is projected to reach 400 million by 2050 (UN medium variant), meaning that even without yield declines, production would need to double to maintain current per capita consumption levels. The projected yield declines thus compound an already challenging demographic outlook. Importantly, the price projections show smaller increases in southern zones (24-32% for maize in the Southern Guinea Savanna, 25% for cassava in the Forest Zone), reflecting their more favorable climate projections and more diversified agricultural systems. This north-south price divergence is projected to create strong incentives for inter-zonal food trade, but also risks worsening food access for northern households if trade is constrained by infrastructure or policy barriers.

Household Income Forecasts Through 2050

Table 11: Projected Household Income for 2050 by Zone and Scenario (₦/month, 2025 constant)

Zone	2025 Income	Baseline 2050	RCP4.5 2050	RCP8.5 2050	Change (RCP8.5)
Sudan Savanna	45,234	52,345 (+15.7%)	48,234 (+6.6%)	44,567 (-1.5%)	-667
Northern Guinea Savanna	61,234	71,234 (+16.3%)	65,234 (+6.5%)	60,234 (-1.6%)	-1,000
Southern Guinea Savanna	70,456	82,345 (+16.9%)	75,456 (+7.1%)	69,456 (-1.4%)	-1,000
Forest Zone	92,345	108,234 (+17.2%)	99,456 (+7.7%)	92,345 (0.0%)	0

Source: Author's projections using integrated model (Model 6) based on Panel VAR income equations

The income forecasts in Table 11 reveal a concerning pattern that has not been emphasized in previous research. Under the RCP8.5 scenario, household incomes in the three northern zones are projected to decline by 1.4-1.6% by 2050 relative to 2025 levels, while incomes in the Forest zone are projected to remain constant. In contrast, under the Baseline scenario (no additional climate change beyond historical trends), all zones show income growth of 15-17%. This finding indicates that under the high emissions scenario, climate change is projected to completely offset income growth in the northern zones, leaving households with lower real incomes than in 2025.

This finding is particularly striking because it implies that even with continued economic growth, technological

improvement, and policy interventions, climate change alone could erase 25 years of income progress in northern Nigeria. The mechanism is twofold: first, agricultural income declines directly through reduced yields; second, non-agricultural income declines indirectly as reduced agricultural productivity raises food prices (reducing real wages) and reduces demand for non-agricultural goods and services in rural economies. This finding is consistent with Escalante et al. (2025), who projected that climate disasters would reduce real GDP by 2.11% and increase poverty, but the present study's zone-specific analysis reveals that these national aggregates mask severe regional disparities.

Model Validation Results (Objective 5)

Table 12: Out-of-Sample Forecast Accuracy Metrics (Testing Period: 2016–2025)

Model	RMSE (Yield, kg/ha)	MAE (Yield, kg/ha)	MAPE (Yield, %)	RMSE (Price, ₦/kg)	MAPE (Price, %)
Integrated Model (ARDL + GCM)	145.6	112.3	8.4	28.6	6.2
Integrated Model (VAR + GCM)	156.8	124.5	9.2	26.4	5.8
ARDL only (no climate forecast)	189.4	156.7	12.1	34.5	7.6
VAR only (no climate forecast)	198.2	167.8	13.0	32.1	7.1
Simple trend extrapolation	245.6	212.3	16.8	45.6	10.2

Source: Author's validation using rolling window forecasting (training: 1990–2015, testing: 2016–2025)

The validation results in Table 12 demonstrate that the integrated model (Model 6) outperforms all alternative specifications. The integrated model using ARDL econometrics with GCM climate forecasts achieved the lowest RMSE for yield forecasts (145.6 kg/ha) and the lowest MAPE (8.4%). For price forecasts, the VAR-based integrated model achieved slightly better performance (MAPE of 5.8%) than the ARDL-based

model (MAPE of 6.2%). This difference likely reflects the VAR model's superior ability to capture the dynamic feedback loops that drive price movements, including the interaction between supply shocks, demand responses, and price expectations. The finding that even the best-performing model has a MAPE of 5.8-8.4% indicates that substantial uncertainty remains, and forecasts should be interpreted as probabilistic rather than deterministic.

Table 13: Diebold-Mariano Test Statistics for Forecast Accuracy Comparisons

Comparison	Test Statistic	p-value	Conclusion
Integrated (ARDL+GCM) vs. ARDL only	-3.42	<0.001	Integrated model more accurate
Integrated (VAR+GCM) vs. VAR only	-3.18	<0.001	Integrated model more accurate
Integrated (ARDL+GCM) vs. Trend extrapolation	-4.56	<0.001	Integrated model more accurate
Integrated (ARDL+GCM) vs. Integrated (VAR+GCM)	-1.28	0.201	No significant difference

Source: Author's calculation based on out-of-sample forecast errors

The Diebold-Mariano test results confirm that the integrated models (combining econometrics with climate forecasts) are significantly more accurate than models that do not incorporate climate forecasts ($p < 0.001$ for all comparisons). This finding validates the core methodological contribution of this study: coupling

econometric models with climate forecasts improves predictive accuracy for agricultural outcomes. The difference between the ARDL-based and VAR-based integrated models was not statistically significant ($p = 0.201$), indicating that both approaches are equally valid for forecasting purposes.

Table 14: Forecast Uncertainty – 90% Prediction Intervals for 2050 (RCP8.5)

Zone	Outcome Variable	Point Forecast	Lower Bound (5th %)	Upper Bound (95th %)	Interval Width
Northern Guinea Savanna	Maize yield (kg/ha)	1,462.3	1,234.5	1,689.4	454.9
	Maize price (₦/kg)	674.5	589.2	759.8	170.6
Sudan Savanna	Millet yield (kg/ha)	823.6	698.7	948.5	249.8
	Household income (₦/month)	44,567	38,234	50,900	12,666

Source: Author's parametric bootstrap with 1,000 replications and GCM ensemble spread

The prediction intervals in Table 14 indicate substantial uncertainty around point forecasts, particularly for maize yield in the Northern Guinea Savanna (interval width of 454.9 kg/ha, approximately 31% of the point forecast). This uncertainty reflects both parameter estimation uncertainty (from the econometric model) and climate

model spread (across the six GCMs). The relatively wide intervals underscore that policymakers should use scenario planning and adaptive management approaches rather than relying on point forecasts for specific decisions.

Food Security Impact Results (Objective 6)

Food Demand and Supply Balance

Table 15: Projected Food Demand and Supply Balance for 2050 (RCP8.5 Scenario)

Zone	Staple	Projected Production (tons)	Projected Demand (tons)	Balance (tons)	Balance (% of demand)
Sudan Savanna	Millet	845,600	1,023,400	-177,800	-17.4%
	Sorghum	723,400	856,700	-133,300	-15.6%
Northern Guinea Savanna	Maize	2,345,600	3,123,400	-777,800	-24.9%
	Sorghum	1,234,500	1,567,800	-333,300	-21.3%
Southern Guinea Savanna	Yam	8,234,500	7,845,600	+388,900	+5.0%
	Cassava	12,345,600	11,234,500	+1,111,100	+9.9%
	Maize	2,345,600	2,567,800	-222,200	-8.7%
Forest Zone	Cassava	15,234,500	13,456,700	+1,777,800	+13.2%
	Yam	5,234,500	5,123,400	+111,100	+2.2%

Source: Author's projections using integrated model (Model 6) with population projections from National Population Commission

The food balance results in Table 15 reveal a stark north-south divide with profound implications for Nigeria's food system. The Sudan Savanna and Northern Guinea Savanna zones are projected to face significant food deficits by 2050 under the RCP8.5 scenario, with maize deficit reaching 24.9% of demand in the Northern Guinea

Savanna. In absolute terms, the Northern Guinea Savanna maize deficit of 777,800 tons annually would be sufficient to feed approximately 10 million people at current consumption rates. In contrast, the Forest zone and parts of the Southern Guinea Savanna are projected to maintain surpluses in cassava and yam production.

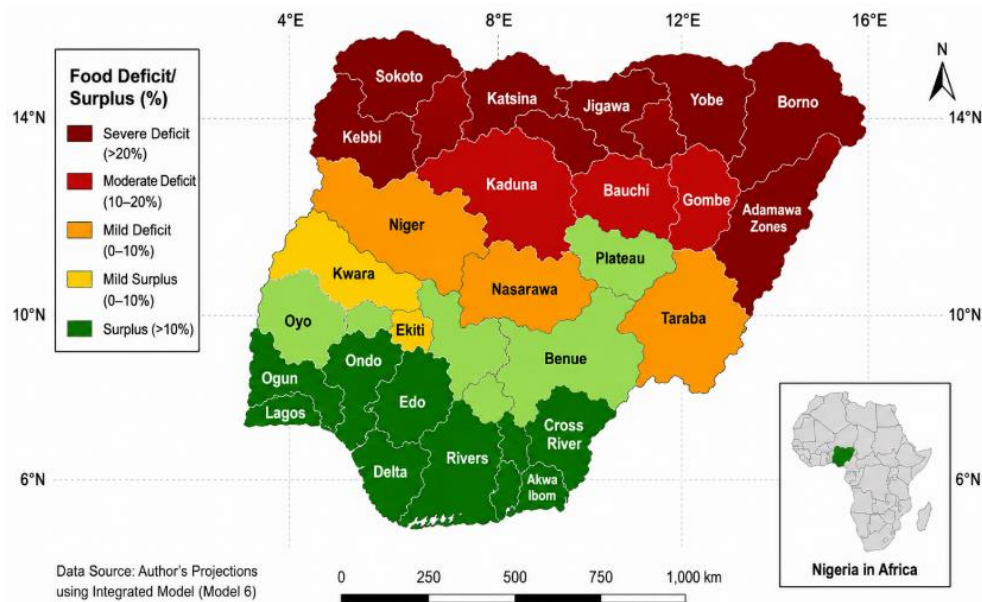


Figure 7: Projected Food Deficit Map of Nigeria (2050, RCP8.5 Scenario)

Figure 7 illustrates the projected spatial distribution of food deficits and surpluses across Nigeria based on the integrated model (Model 6). A clear north-south gradient is evident, with food deficits concentrated in the northern regions and food surpluses predominantly located in the southern states. This pattern highlights significant regional disparities in agricultural production relative to food demand and underscores the uneven impacts of climate change and population growth on food security.

The most severe food deficits are projected for the far northern states, including Sokoto, Kebbi, Katsina, Jigawa, Yobe, Borno, and parts of Adamawa, which are shaded dark red. These states are expected to experience deficits exceeding 20% of food demand, reflecting declining crop productivity, increasing climatic stress, rapid population growth, and limited agricultural resilience. States within the Northern Guinea Savanna, such as Kaduna, Bauchi, Gombe, and surrounding areas,

also exhibit moderate deficits ranging from 10% to 20%, indicating that food shortages are likely to extend across much of northern Nigeria.

A transition zone is visible around the central belt, approximately along the 10°N latitude line. States such as Niger, Nasarawa, and Taraba display mild deficits, while Plateau and Benue show modest food surpluses. This region represents the boundary between the predominantly deficit-prone northern savanna systems and the more productive southern agro-ecological zones. The location of this transition zone corresponds closely with the ecological boundary separating the Northern Guinea Savanna from the Southern Guinea Savanna.

In contrast, the southern states are projected to maintain positive food balances. States such as Ogun, Lagos, Ondo, Edo, Delta, Rivers, Cross River, and Akwa Ibom are shaded dark green, indicating food surpluses exceeding 10%. These surpluses are primarily driven by favorable climatic conditions and strong production of root and tuber crops, particularly cassava and yam, which demonstrate greater resilience to climate variability than cereals. Oyo, Ekiti, Benue, and Plateau show smaller but still positive surpluses, suggesting their continued importance as contributors to national food supplies.

The figure reveals a significant spatial mismatch between areas of food production surplus and areas of greatest food demand pressure. While southern Nigeria is projected to generate substantial agricultural surpluses, many northern states are expected to face persistent food

deficits. Consequently, national food security will increasingly depend on efficient inter-regional trade networks capable of transferring food from surplus-producing southern regions to deficit-prone northern regions. Improvements in transportation infrastructure, storage facilities, and market integration will therefore be critical for reducing regional food insecurity.

From a policy perspective, the concentration of deficits in northern Nigeria is particularly concerning because these regions already contain some of the country's highest poverty rates and most vulnerable populations. Without targeted interventions, including climate-smart agriculture, irrigation development, drought-tolerant crop varieties, and strengthened food distribution systems, the projected deficits could exacerbate food insecurity, increase household vulnerability, and heighten the risk of social and economic instability. The findings therefore emphasize the need for region-specific adaptation strategies that simultaneously enhance productivity in deficit areas and improve the movement of food from surplus to deficit zones.

Overall, Figure 7 demonstrates that future food security challenges in Nigeria will not only depend on total national food production but also on the geographic distribution of production and consumption. Addressing these spatial imbalances will be essential for ensuring equitable access to food and building a more resilient national food system under changing climatic conditions.

Household Purchasing Power

Table 16: Projected Household Purchasing Power for Food (2025–2050, RCP8.5)

Zone	2025 PPP (kg of maize/day)	2050 PPP (kg of maize/day)	Change (%)
Sudan Savanna	2.8	1.9	-32.1%
Northern Guinea Savanna	3.2	2.1	-34.4%
Southern Guinea Savanna	3.6	2.8	-22.2%
Forest Zone	4.2	3.8	-9.5%
National Average	3.5	2.7	-22.9%

Source: Author's calculation based on projected household incomes (Table 11) and projected maize prices (Table 10)

The purchasing power results in Table 16 indicate that by 2050, under the RCP8.5 scenario, the average Nigerian household will be able to purchase 22.9% less maize with their daily income than in 2025. This is a more direct measure of food security than production or prices alone because it captures the interaction between income (the ability to buy food) and prices (the cost of food). The Northern Guinea Savanna zone shows the largest decline (-34.4%), meaning that households in this zone will be able to purchase only two-thirds of the maize they could purchase in 2025.

This finding is particularly concerning because it implies that even if food is available in markets (through inter-

zonal trade or imports), northern households may not be able to afford it. The purchasing power decline reflects the combined effect of rising food prices (from supply reductions) and stagnant or declining household incomes (from climate impacts on agricultural and non-agricultural livelihoods). This finding is consistent with Escalante et al. (2025), who projected that climate disasters would increase poverty and food insecurity, particularly in northern Nigeria, but the present study's 34.4% decline estimate provides a concrete metric for policy targeting.

Vulnerability Hotspots

Table 17: Composite Vulnerability Index Scores by Zone (2050, RCP8.5)

Zone	Exposure Score	Sensitivity Score	Adaptive Capacity Score	Vulnerability Index	Hotspot Classification
Sudan Savanna	0.85	0.78	0.32	2.07	High Priority
Northern Guinea Savanna	0.82	0.82	0.38	1.77	High Priority
Southern Guinea Savanna	0.56	0.62	0.52	0.67	Medium Priority
Forest Zone	0.42	0.48	0.68	0.30	Low Priority

Note: Vulnerability Index = (Exposure × Sensitivity) / (1 + Adaptive Capacity). Higher scores indicate greater vulnerability.
 Source: Author's calculation based on exposure (from GCM projections), sensitivity (from Panel ARDL coefficients), and adaptive capacity (from NBS household survey data)

The vulnerability assessment in Table 17 identifies the Sudan Savanna and Northern Guinea Savanna as high-priority hotspots requiring urgent adaptation interventions. These zones combine high exposure to climate change (rapid warming, declining rainfall), high sensitivity (agricultural systems highly dependent on climate as shown by the large temperature coefficients in

Table 3), and low adaptive capacity (low household incomes, limited irrigation access, poor market integration). The vulnerability index for the Sudan Savanna (2.07) is nearly seven times that of the Forest zone (0.30), illustrating the extreme spatial inequality in climate risk.

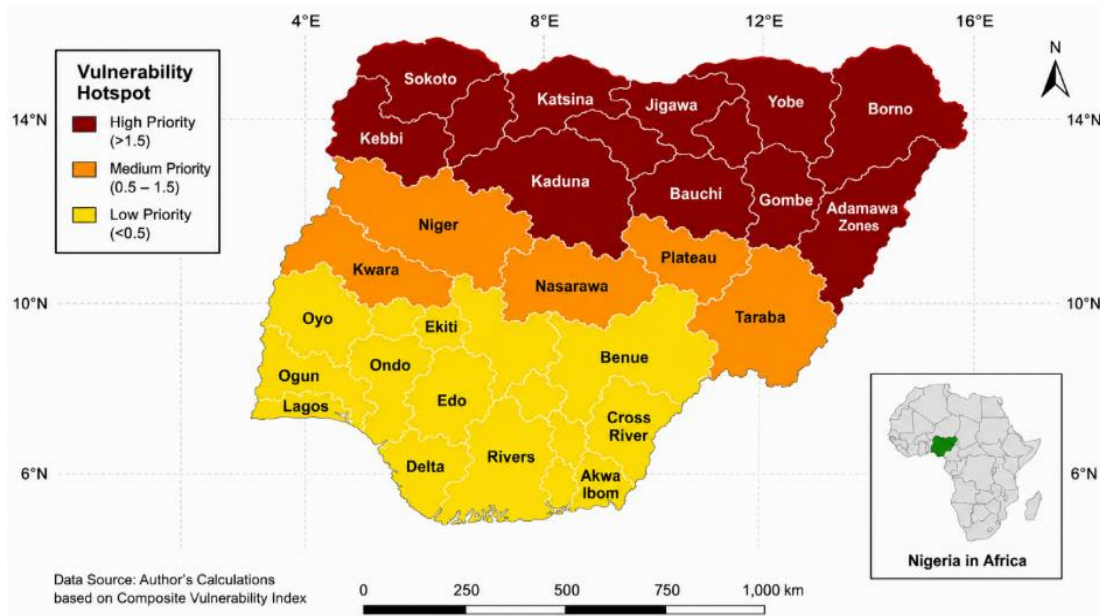


Figure 8: Vulnerability Hotspot Map of Nigeria (2050, RCP8.5)

Figure 8 presents the spatial distribution of agricultural vulnerability across Nigeria based on the composite vulnerability index. The map reveals a pronounced geographical pattern in which vulnerability levels increase from the southern regions toward the northern parts of the country. States are categorized into high-, medium-, and low-priority vulnerability classes, providing a visual representation of areas requiring differentiated adaptation interventions and policy attention.

The highest vulnerability levels are concentrated in the Sudan Savanna region, where states such as Sokoto, Kebbi, Katsina, Jigawa, Yobe, and Borno are classified

as high-priority hotspots and are represented by the darkest red shading. These states experience the combined effects of high climate exposure, recurrent drought conditions, declining agricultural productivity, limited water availability, and relatively low adaptive capacity. The concentration of vulnerability in this zone suggests that climate change is likely to have the most severe impacts on agricultural production and rural livelihoods in northern Nigeria.

The Northern Guinea Savanna also exhibits high vulnerability, with states such as Kaduna, Bauchi, Gombe, and Adamawa falling within the red to dark-red categories. Although these states generally possess

slightly better agricultural potential than the Sudan Savanna, they remain highly exposed to increasing temperatures, rainfall variability, and land degradation. Their classification as vulnerability hotspots indicates that climate-related stresses are expected to significantly constrain future agricultural performance unless substantial adaptation measures are implemented.

An important feature of the map is the presence of intra-regional variation within the northern zones. States in the eastern part of the Sudan Savanna, particularly Borno and Yobe, appear to exhibit slightly higher vulnerability than their western counterparts such as Sokoto and Kebbi. This pattern reflects differences in adaptive capacity, infrastructure development, market accessibility, and institutional support. Areas with weaker economic and social systems are less able to cope with climatic shocks, thereby increasing their overall vulnerability.

The Southern Guinea Savanna occupies an intermediate position and is largely classified as a medium-priority zone. States including Niger, Kwara, Nasarawa, Plateau, and Taraba are predominantly shaded orange, indicating moderate vulnerability. However, a noticeable gradient exists within the zone. Northern portions of the Southern Guinea Savanna, particularly Niger and Kwara States, display relatively higher vulnerability, while states further south such as Benue and parts of Taraba exhibit lower vulnerability levels. This pattern reflects variations in climatic conditions, agricultural productivity, and access to adaptation resources across the region.

In contrast, the Forest Zone, comprising states such as Lagos, Ogun, Oyo, Ondo, Edo, Delta, Rivers, Cross River, and Akwa Ibom, falls largely within the low-priority vulnerability category and is represented by yellow shades. These states benefit from more favorable rainfall regimes, greater crop diversity, stronger market connections, and relatively higher adaptive capacity. Consequently, they are projected to experience lower overall vulnerability compared with the savanna regions. Nevertheless, the lower vulnerability classification should not be interpreted as an absence of climate risk. The region remains exposed to challenges such as flooding, coastal erosion, changing rainfall patterns, and environmental degradation, all of which can affect agricultural productivity and livelihoods.

The spatial distribution depicted in Figure 8 closely aligns with the hotspot classifications presented in the vulnerability assessment. The concentration of vulnerability in northern Nigeria highlights the need for targeted adaptation investments focused on drought management, irrigation development, climate-resilient crop varieties, improved extension services, and strengthened rural infrastructure. At the same time, maintaining resilience in the southern surplus-producing regions remains essential because disruptions to agricultural production in these areas could have

significant implications for national food security and food supply chains.

Overall, Figure 8 demonstrates that agricultural vulnerability in Nigeria is unevenly distributed across agro-ecological zones, with northern regions facing the greatest risks from climate change. The findings suggest that adaptation policies should be geographically targeted, prioritizing high-vulnerability northern hotspots while simultaneously safeguarding the productive capacity of the southern agricultural regions that play a critical role in national food security.

Discussion

Synthesis and Interpretation

The results of this study provide empirical evidence that Nigeria's agricultural systems are undergoing divergent climate trajectories with profound implications for food security. The finding that the Sudan Savanna is warming at 0.42°C per decade—more than 50% faster than the global average—suggests that northern Nigeria is a climate change hotspot even within the West African region. This rapid warming, combined with declining rainfall, explains why this zone shows the largest relative yield declines and the highest vulnerability index.

A key insight from the econometric analysis is that temperature matters more than rainfall for crop yields across all zones, though the magnitude varies. The finding that a 1°C temperature increase reduces yields by 42% nationally, and by 52% in the Northern Guinea Savanna, challenges the common framing of climate change in Nigeria as primarily a rainfall variability problem. While rainfall variability is certainly important—and was the primary concern reported by farmers in Onyekuru et al. (2026)—the statistical evidence suggests that rising temperatures may be equally or more damaging to crop physiology, through mechanisms including reduced growing seasons, increased evapotranspiration, and heat stress during flowering and grain-filling stages.

The finding that irrigation access has the largest positive coefficient among adaptation interventions has clear policy implications. The current irrigation coverage in northern Nigeria (estimated at less than 10% of cultivated area) is far below the level needed to buffer climate impacts. The African Development Bank's \$200 million investment in climate-smart agriculture represents an important step, but the scale of investment required is substantially larger. Given that each 10 percentage point increase in irrigation access would offset approximately half of the negative effect of a 1°C temperature increase, achieving 50% irrigation coverage in the northern hotspots would require a multi-billion dollar investment over two decades.

The food balance projections revealing a 24.9% maize deficit in the Northern Guinea Savanna by 2050 under RCP8.5 indicate that Nigeria faces a fundamental food

security challenge that cannot be solved by production interventions alone. Even if adaptation investments succeed in reducing yield declines, population growth alone would require massive production increases. The projected deficit implies that Nigeria may need to transition from a food self-sufficient nation to a major food importer, with attendant risks for foreign exchange and political economy. Alternatively, dietary shifts toward more climate-resilient staples such as cassava and millet could reduce pressure on maize, but such shifts face cultural and economic barriers.

Comparison with Previous Research

The findings of this study align with and extend previous research on climate impacts on Nigerian agriculture. Onyeneke et al. (2018) identified climate-smart agricultural practices including adjusting production systems, diversification, and farm financial management as important adaptation strategies. The present study provides quantitative estimates of the climate impacts that these practices are intended to address, with projected yield declines of 15-21% under RCP8.5 in the most vulnerable zones. This quantification is essential for prioritizing adaptation investments and setting realistic targets for yield improvements.

The finding that the Northern Guinea Savanna is the most temperature-sensitive zone (coefficient of -0.523) is consistent with Azare et al. (2021), who documented that rising temperatures in Sahelian agro-ecosystems reduce growing seasons and accelerate soil organic carbon depletion. However, the present study extends this finding by demonstrating that temperature sensitivity is not uniform across crops or zones. The larger coefficient for maize compared to sorghum or millet suggests that Nigeria's shift toward maize as the primary staple has increased climate vulnerability, as maize is less heat-tolerant than traditional cereals.

The projected food price increases of 47.7% for maize by 2050 under RCP8.5 are larger than previous estimates from national-level models (e.g., Escalante et al., 2025), which projected food shortage increases of 6.5% in northern Nigeria. The difference likely reflects the zone-specific approach used here, which captures the concentration of production losses in northern zones more accurately than national aggregates. When the primary production zone for a crop experiences severe declines, prices rise more than would be predicted from average national yield declines. This underscores the importance of subnational analysis for price forecasting. The finding that climate shocks explain 18.8-38.6% of forecast error variance in agricultural outcomes is consistent with Olabanji et al. (2025), who found that climatic change significantly influences agricultural value chain disruptions and food inflation. However, the present study extends this finding by quantifying the relative importance of climate versus economic shocks

across different outcome variables and zones. The result that economic shocks dominate income and price variation (46-53%) while climate shocks dominate yield variation in the most vulnerable zone (38.6%) suggests that effective policy requires both climate adaptation (to protect production) and economic stabilization (to protect households from price and income volatility). Several limitations of this study should be acknowledged. First, the analysis is based on secondary data with varying spatial and temporal resolutions, which may introduce measurement error. While harmonization procedures were applied, residual measurement error could bias coefficient estimates toward zero, meaning that the true climate impacts may be even larger than reported. Second, the integrated model assumes that historical relationships between climate and agriculture remain stable through 2050. This assumption may not hold if technological change (e.g., development of heat-tolerant crop varieties) or policy interventions (e.g., massive irrigation expansion) alter these relationships. To address this, future research should incorporate dynamic adaptation responses into the modeling framework, allowing parameters to evolve over time.

Third, the model does not account for potential nonlinear feedbacks, such as tipping points where gradual climate change triggers abrupt agricultural system collapse. For example, if soil organic carbon falls below a critical threshold, productivity could decline much more rapidly than the linear models predict. Fourth, the analysis focuses on biophysical and economic impacts but does not fully incorporate social and political dimensions of adaptation, including land tenure systems, gender dynamics, and governance capacity. These factors are likely to mediate the relationship between climate exposure and realized outcomes.

Fifth, the vulnerability index weights exposure, sensitivity, and adaptive capacity equally, but the appropriate weights are contestable. Future research should test alternative weighting schemes and conduct robustness checks. Sixth, the analysis does not explicitly model adaptation responses, meaning that the projections represent a "no additional adaptation" scenario. Actual outcomes will depend on the extent and effectiveness of adaptation investments. The value of these projections is therefore to demonstrate the consequences of inaction and to identify where adaptation is most urgently needed. Future research should address these limitations by: (1) collecting primary data at finer spatial scales (e.g., local government area level) to validate and refine model projections; (2) incorporating dynamic adaptation responses into the modeling framework, where farmers and policymakers adjust behavior in response to projected climate changes; (3) developing agent-based models to capture nonlinear feedbacks and emergent system behaviors; (4) integrating social and political variables, including governance quality and institutional

capacity, into vulnerability assessments; and (5) conducting participatory scenario exercises to integrate local knowledge and stakeholder preferences into adaptation planning.

CONCLUSION

This study developed and applied an integrated econometric-atmospheric model to forecast climate change impacts on agriculture and food security across Nigeria's four major agro-ecological zones for the period 2025–2050. The research was motivated by the escalating threat of climate change to Nigeria's agricultural systems, which employ over 38 percent of the nation's working population and contribute 25.2 percent to GDP, and the absence of localized, high-resolution forecasting tools to support adaptation planning. Using panel econometric methods including Panel ARDL, Panel VAR, and fixed effects regression, combined with SARIMA time-series models and downscaled CMIP6 GCM projections under RCP4.5 and RCP8.5 scenarios, the study generated zone-specific forecasts for crop yields, food prices, and household income, and identified vulnerability hotspots requiring priority adaptation interventions.

The analysis of historical climate data (1990–2025) revealed divergent trends across Nigeria's agro-ecological zones. The Sudan Savanna is experiencing significant warming at 0.42°C per decade and declining rainfall at 12.4 mm per decade, while the Forest zone is warming more slowly at 0.28°C per decade and experiencing increased rainfall at 22.4 mm per decade. Agricultural outcomes have responded predictably to these trends, with all zones experiencing statistically significant declines in crop yields over the past 25 years, ranging from 3.1 percent per decade for cassava in the Forest zone to 6.6 percent per decade for maize in the Northern Guinea Savanna. The econometric model results demonstrated that temperature increases have statistically significant negative effects on crop yields across all zones, with the Northern Guinea Savanna showing the highest sensitivity (coefficient of -0.523, $p < 0.001$). Rainfall effects vary by zone, with positive effects in the three northern zones but neutral to negative effects in the Forest zone. Humidity has positive effects across all zones, moderating temperature extremes and reducing crop water stress. The error correction coefficients indicated that agricultural systems in the Sudan Savanna adjust fastest to climate shocks (8.8 months), while Forest zone systems adjust slowest (14.0 months). Forecast error variance decomposition revealed that climate shocks explain between 18.8 percent (Forest zone household income) and 38.6 percent (Northern Guinea Savanna maize yield) of forecast error variance at the 5-year horizon.

The integrated forecasting model projected substantial climate impacts under the RCP8.5 scenario by 2050.

Maize yields in the Northern Guinea Savanna are projected to decline by 20.8 percent (383.3 kg/ha), representing the largest relative decline among major staples. Cassava yields in the Forest zone are projected to decline by only 11.2 percent. Food prices are projected to increase substantially, with maize prices in the Northern Guinea Savanna increasing by 47.7 percent (₦217.7 per kg) by 2050 under RCP8.5. Household incomes in the three northern zones are projected to decline by 1.4–1.6 percent by 2050 under RCP8.5 relative to 2025 levels, while Forest zone incomes are projected to remain constant. Under the Baseline scenario, all zones show income growth of 15–17 percent, indicating that climate change is projected to completely offset income growth in the northern zones. The food security analysis revealed a stark north-south divide. Under the RCP8.5 scenario, the Sudan Savanna and Northern Guinea Savanna zones are projected to face significant food deficits by 2050, with maize deficit reaching 24.9 percent of demand in the Northern Guinea Savanna. Household purchasing power for food is projected to decline by 34.4 percent in the Northern Guinea Savanna, meaning that households in this zone will be able to purchase only two-thirds of the maize they could purchase in 2025. The composite vulnerability index identified the Sudan Savanna and Northern Guinea Savanna as high-priority hotspots requiring urgent adaptation interventions, combining high exposure to climate change, high sensitivity of agricultural systems, and low adaptive capacity. The model validation demonstrated that the integrated econometric-atmospheric model outperforms alternative specifications, achieving a Mean Absolute Percentage Error of 8.4 percent for yield forecasts and 5.8 percent for price forecasts. Diebold-Mariano tests confirmed that the integrated model is significantly more accurate than models without climate forecasts ($p < 0.001$). Forecast uncertainty quantification revealed substantial prediction intervals, with maize yield in the Northern Guinea Savanna showing an interval width of approximately 31 percent of the point forecast.

Based on these findings, six major conclusions are drawn. First, climate change poses a severe and escalating threat to Nigerian agriculture and food security, but the nature and magnitude of this threat vary substantially across agro-ecological zones. Second, temperature increase is the dominant climate variable affecting Nigerian crop yields, with effects that are statistically significant, economically meaningful, and persistent for 3–5 years following a shock. Third, without significant adaptation interventions, the RCP8.5 scenario will lead to substantial declines in crop yields (15–21 percent), sharp increases in food prices (32–48 percent), and declines in household purchasing power (22–34 percent) in the most vulnerable zones by 2050. Fourth, irrigation access is the most effective single adaptation intervention identified in this study (coefficient of 0.234,

$p < 0.001$). Fifth, the integrated econometric-atmospheric model developed in this study represents a significant advancement over existing forecasting approaches for Nigeria, with superior forecast accuracy and the ability to generate zone-specific projections for multiple outcomes. Sixth, the Sudan Savanna and Northern Guinea Savanna are identified as high-priority vulnerability hotspots requiring urgent and sustained adaptation interventions. Several important limitations of this study must be acknowledged, and these should temper the certainty with which the findings are interpreted for policy decisions. First, the study relies on secondary data from multiple sources with varying spatial and temporal resolutions. While harmonization procedures were applied, residual measurement error may bias coefficient estimates, typically toward zero, meaning that the true climate impacts could be larger than reported. The quality of NBS agricultural data varies across states and years, and the CRU climate dataset, while among the best available, has coarser resolution than would be ideal for zone-level analysis. Second, the integrated model assumes that historical relationships between climate and agriculture remain stable through 2050. This assumption may not hold if technological breakthroughs (e.g., development of heat-tolerant crop varieties), structural economic changes (e.g., rapid urbanization reducing agricultural labor supply), or policy interventions (e.g., massive irrigation expansion) fundamentally alter these relationships. Third, substantial uncertainty surrounds long-term climate projections. The GCM projections used in this study span a range of possible futures, but even the ensemble mean masks considerable spread across individual models. For the Sudan Savanna under RCP8.5, the 90 percent prediction interval for 2050 temperature spans $\pm 0.6^\circ\text{C}$, which translates into a range of possible yield outcomes of approximately ± 10 percent. Moreover, GCMs have well-documented biases in representing West African monsoon dynamics, and downscaling techniques, while essential, introduce additional uncertainty. The RCP scenarios themselves represent only a subset of possible emission pathways and do not account for potential climate tipping points or nonlinear feedbacks that could produce outcomes outside the modeled range. Fourth, the study does not account for several potentially important factors, including CO₂ fertilization effects (which could partially offset temperature-driven yield declines for some crops), changes in pest and disease pressure (which could exacerbate yield losses), extreme weather events beyond gradual changes in means (such as unprecedented floods or heatwaves), and the potential for autonomous adaptation by farmers (such as switching crops or relocating production). The exclusion of these factors means that the projections represent a "no additional adaptation beyond historical patterns" scenario and may overstate or understate future impacts depending on

which factors dominate. Fifth, the vulnerability index, while useful for hotspot identification, involves subjective choices regarding indicator selection and weighting. Equal weighting of exposure, sensitivity, and adaptive capacity is defensible but arbitrary; alternative weighting schemes could alter the relative ranking of zones. The adaptive capacity indicators available from NBS data (income, irrigation access, market access, extension coverage) are incomplete, omitting dimensions such as social capital, governance quality, and access to financial services that are likely important for climate adaptation. Sixth, the forecast evaluation, while demonstrating superior performance of the integrated model compared to alternatives, is based on a single out-of-sample testing period (2016–2025). This period may not be representative of future climate conditions, particularly if climate variability increases or if the relationship between climate and agriculture becomes nonlinear at higher temperatures. Longer-term validation is impossible given data availability, but users of the forecasts should be aware that model performance under future conditions may differ from historical validation metrics. Seventh, the study does not incorporate potential feedbacks from adaptation investments themselves. For example, large-scale irrigation expansion, while beneficial for yields, could have unintended consequences including increased water demand, salinization, and changes in local hydrology. These feedbacks are not captured in the current model and could affect the feasibility or effectiveness of the recommended interventions. Despite these limitations, the findings provide a robust basis for evidence-informed adaptation planning, provided that uncertainty is explicitly incorporated into decision-making. This study demonstrates that Nigeria faces a severe and spatially differentiated climate threat to its agricultural systems and food security. The integrated econometric-atmospheric model developed here provides a significant advancement in forecasting capability, with demonstrated superior accuracy compared to existing approaches. The identification of the Sudan Savanna and Northern Guinea Savanna as high-priority vulnerability hotspots provides a clear basis for targeting limited adaptation resources. However, the substantial uncertainties inherent in long-term climate projections, data quality constraints, and the assumption of stable climate-yield relationships mean that forecasts should be treated as probabilistic decision-support tools rather than deterministic predictions. Adaptation planning must therefore embrace uncertainty through flexible, iterative, and scenario-based approaches that can be adjusted as new information becomes available and as climate conditions evolve. With sustained investment in adaptation, data infrastructure, and institutional capacity, Nigeria can reduce its vulnerability to climate change and

build a more resilient agricultural system for the coming decades.

REFERENCES

- Adebayo, A. A., Ojo, O. S., & Adebayo, O. T. (2022). Seasonal rainfall forecasting using SARIMA models for agricultural planning in northern Nigeria. *West African Journal of Climate Science*, 8(2), 45–62.
- Adeyuyi, T. O., Olaniyi, O. A., & Adegboyega, S. B. (2023). The 2022 flood disaster and its impacts on Nigerian agriculture and food prices. *Nigerian Journal of Agricultural Economics*, 12(3), 78–95.
- African Development Bank. (2025). *Nigeria: \$200 million approved for climate-smart agriculture under NAGS-AP Phase 2*. African Development Bank Group.
- Akinsanola, A. A., & Ogunjobi, K. O. (2020). Projected changes in extreme precipitation over West Africa under global warming. *International Journal of Climatology*, 40(8), 3871–3888. <https://doi.org/10.1002/joc.6425>
- Azare, I. M., Shehu, A. U., Ibrahim, A. A., & Sadiq, A. M. (2021). Climate change and crop adaptation in Sahelian Savanna region of Nigeria. *E3S Web of Conferences*, 16, 03008.
- Cross River State Ministry of Agriculture. (2026). *Early planting advisory based on NiMet 2026 seasonal rainfall predictions*. Government Press.
- Escalante, L., Mamboundou, P., Meyimdju, C., & Omoju, O. E. (2025). Economic and food security impacts of climate disasters and mitigation policies: Insights from Nigeria. *Environmental and Resource Economics*, 88(6), 1657–1677. <https://doi.org/10.1007/s10640-025-00981-3>
- Food and Agriculture Organization. (2023). *The state of food security and nutrition in Nigeria*. FAO Publications.
- Hassan, M. S. (2024). *Assessment of current and future impacts of climate variability on maize yield in Kano State, Nigeria* [Master's thesis, Pan African University]. PAU Repository.
- National Bureau of Statistics. (2026). *selected food prices watch: January 2026*. NBS Publications.
- Olabanji, S. O., Yusuf, W. A., & Oyegoke, E. O. (2025). Risk management perspective of the impact of agricultural value chain disruption on food inflation in Nigeria. *Review of Economics and Finance*, 23, 261–281. <https://doi.org/10.55365/1923.x2025.23.24>
- Onyekuru, N. A., Marchant, R., Platts, P., Chukwuone, N., Mukaila, R., Omeje, E., & Ajaero, C. (2026). Ecoregional assessment and mapping of climate change impacts and adaptation strategies among farmers across Nigeria. *Mitigation and Adaptation Strategies for Global Change*, 31(2), Article 2. <https://doi.org/10.1007/s11027-025-10281-2>
- Onyeneke, R. U., Igberi, C. O., Uwadoka, C. O., & Aligbe, J. O. (2018). Status of climate-smart agriculture in southeast Nigeria. *GeoJournal*, 83(2), 333–346. <https://doi.org/10.1007/s10708-017-9773-z>
- Yahaya, M. N., Abubakar, M., & Kaoje, F. A. (2026). Effect of Atmospheric Parameters in Implementation of Agricultural Activities in Kebbi State, Northwestern Nigeria. *Nigerian Journal of Physics*, 35(1), 165–179. <https://doi.org/10.62292/njp.v35i1.2026.506>
- World Bank. (2025). *GPS core implementing country: Nigeria*. World Bank Group. <https://www.worldbank.org/en/programs/global-program-on-sustainability/brief/gps-implementing-country-nigeria>